A Stable Oxygen Isotope Approach to Tropical Cyclone Reconstruction Northeast Queensland, Australia

Renske Löffler

0427063

Department of Geochemistry

Faculty of Geosciences

Utrecht University

Abstract

Long-term high temporal resolution records of tropical cyclone activity are needed to distinguish natural variability from anthropogenically induced changes in tropical cyclone frequency and/or intensity. Existing instrumental and palaeocyclone records are either too short or too coarse in resolution. Stalagmites provide long-term high temporal resolution records which have been proven useful for tropical cyclone reconstructions due to the sensitivity of the isotopic composition of stalagmites to changes in precipitation and other local climate phenomena.

In order to reconstruct tropical cyclones in Northeast Queensland, Australia, a stalagmite and a peat core were analyzed. This study presents two climate records: a 220 year sediment record (1778-1997) from Quincan Crater (peat core Qui-1) and a 105 year stalagmite record (1901-2005) from Chillagoe Caves (CH2). Climate reconstructions from these records were compared to instrumental climate data such as precipitation, temperature, and tropical cyclone activity, in order to test the suitability of these samples for reconstructing tropical cyclones within the study area.

Temperature reconstructions by branched glycerol dialkyl glycerol tetraether membrane lipid content in sediment samples show a close match with summer temperatures. Oxygen isotope measurements on calcite samples from the stalagmite correlate positively with tropical cyclone frequency. The oxygen isotopes correlate with carbon isotopes, possibly due to a similar environmental control on both isotopic records. Sea surface temperatures in the Niño-4 area (5°S-5°N; 160°E-150°W) and the Southern Oscillation Index show some similarities with oxygen and carbon isotopes in accordance with previous studies. CH2 and Qui-1 are both long term high temporal resolution records with a high potential for reconstructing tropical cyclone activity. Further research is needed to establish relationship between tropical cyclones and the isotopic composition of CH2, as well as to test if Qui-1 is influenced by tropical cyclone activity.

Contents

Introduction

Tropical cyclone generation is controlled by environmental factors such as sea surface temperature, surface air pressure , low-level relative vorticity, and deep-tropospheric vertical wind shear (Holland, 1997; Ramsay et al., 2008). It is unlikely for a tropical cyclone to form over an ocean with SST below 26°C, because ocean surface heat serves as the number one energy source for tropical cyclones (Basher and Zheng, 1995; Holland, 1997; Ramsay et al., 2008). Statistical analyses show a significant link between tropical cyclones over eastern Australia and several sea surface temperature related climate oscillations in the South Pacific, such as Interdecadal Pacific Oscillation (IPO), Southern Oscillation Index (SOI) and consequently El Niño Southern Oscillation (ENSO) (Allan, 1988; Chan, 1985; Fan and Liu, 2008; Grant and Walsh, 2001; Nicholls, 1979; Ramsay et al., 2008). Anthropogenic influences on climate have lead to increased sea surface temperatures (Watson, 1996) which could have significant consequences for tropical cyclone genesis and trends in tropical cyclone frequency and/or intensity.

Previous studies which have analyzed trends in tropical cyclone frequency and/or intensity do not give conclusive results about the impact of human activities. Analysis of instrumental records show a decrease in the number of tropical cyclones since 1960, but an increase in their intensity (Nicholls et al., 1998). However, instrumental records have only become reliable after 1970 due to the lack of accurate measurement techniques before that time (Landsea et al., 2006; Nicholls et al., 1998). The records are often slightly improved by the additional use of fairly reliable historical counts (Flay and Nott, 2007). Records are also subject to artificial effects caused by changing cyclone-monitoring methods (Landsea et al., 2006). Models used for tropical cyclone analysis are based on the same limited data and give conflicting results regarding trends in frequency and/or intensity (Emanuel et al., 2008; Flay and Nott, 2007; Walsh and Ryan, 2000). The available datasets are too limited in time to analyze long term trends and separate natural from anthropogenic trends. For an accurate assessment of trends, reliable long-term high temporal resolution palaeotempestological records are needed.

Previous studies in the field of palaeotempestology have developed methods to create long term tropical cyclone records. Storm deposits, such as detrital coral and shell ridges, have been used to reconstruct cyclones of high intensity (Baines and McLean, 1976; Hayne and Chappell, 2001; Nott and Hayne, 2001; Nott, 2003). Hummocky cross-stratification and overwash deposits have also been used to reconstruct palaeotempests (Donnelly et al., 2001a; Donnelly et al., 2001b; Donnelly and Woodruff, 2007; Ito et al., 2001; Liu and Fearn, 2000). The most intense tropical cyclones are most

likely to create clear storm deposits and will erase storm deposits from less intense tropical cyclones. Therefore the above described methods are all limited in temporal resolution.

This study examines a stalagmite and a peat core from Northeast Queensland and assessed their use in reconstructing tropical cyclone activity. Stalagmites and sediment cores can provide accurately dated, high temporal resolution records extending thousands of years into the past. Both contain multiple climate proxies and may be used for tropical cyclone reconstructions based on the isotopic composition of the samples. Before an accurate long term record can be created the samples need to be calibrated with the tropical cyclone database and other instrumental climate records.

Stalagmites are useful for palaeoclimate reconstructions as they incorporate proxies such as isotope signals, trace elements, luminescence and layer thickness. Stalagmites are formed when groundwater percolating down reaches an underground cavern. Here calcite is deposited due to CO_2 degassing or evaporation (Self and Hill, 2003; White, 2007). When deposition occurs by slow CO_2 degassing, isotopic equilibrium is maintained and the isotopic values of the groundwater are recorded (Hendy, 1971; Spötl et al., 2005; White, 2004). During fast CO_2 degassing and/or evaporation the deposition reaction occurs too fast to maintain isotopic equilibrium. ^{16}O and ^{12}C are preferentially lost to the cave atmosphere, leaving the solution and consequently the calcite enriched in ^{18}O and ^{13}C. This fractionation is stronger at the edges of the stalagmite compared to the apex, due to thinner layers at the edges (Hendy, 1971). Based on this process two criteria are widely used as the Hendy test to exclude kinetic fractionation: minimal variation in isotopic composition along the layer (e.g. <0.8‰) and no linear relationship between $\delta^{18}O$ and $\delta^{13}C$ (Hendy, 1971; Hendy and Wilson, 1968). By incorporating $\delta^{18}O$-signals in their seasonally deposited calcite layers, stalagmites record climate information regarding temperature and precipitation.

Stable isotopes in stalagmites can be used for reconstructing tropical cyclone activity in the study area. Tropical cyclone precipitation lowers the $\delta^{18}O$ of lake surface waters and ground water (Frappier, 2008; Lawrence, 1998; Miller et al., 2006; Nott et al., 2007). Rain falling during a tropical cyclone is significantly isotopically depleted (in both $\delta^{18}O$ and δD) compared to rain falling under other conditions due to excessive isotopic fractionation (Gedzelman et al., 2003; Gedzelman and Lawrence, 1982; Lawrence and Gedzelman, 1996; Lawrence et al., 2004; Lawrence et al., 1998). A case study in Texas, USA, shows a mean $\delta^{18}O$ value of -2.9‰ for summer rains and a value of -9.4‰ for tropical cyclones (Lawrence, 1998). Such a depleted isotope signal has been shown to incorporated by in fresh water carbonates (Lawrence, 1998), tree rings (Miller et al., 2006) and stalagmites (Frappier et al., 2007; Nott et al., 2007). This study focuses on the usability of this proxy on a seasonal scale on a stalagmite from Northeast Australia.

Sediment cores contain climate proxies such as branched glycerol dialkyl glycerol tetraether membrane lipids (GDGT's) (Weijers et al., 2007). Branched GDGT's in soil samples have been proven useful in mean annual air temperature (MAT) reconstructions (Weijers et al., 2007). Depending on temperature and pH, GDGT-producing soil bacteria appear to change their membrane lipid composition, adjusting their amount of methyl branches and cyclopentyl moieties (Weijers et al., 2007). In this study the quality of the sediment core as a palaeoclimate record is tested using this proxy and instrumental records.

Environmental Setting

Chillagoe Caves

The Chillagoe limestone region lies 130 km inland from the tropical coastal town of Cairns in Northeast Queensland, Australia (see Figure 1). Highly seasonal rainfall and frequent tropical cyclone activity (see Figure 2) make this area potentially excellently suited for using stalagmites in Chillagoe Caves for tropical cyclone reconstructions. Chillagoe has a complex geological history, with many phases of metamorphosis, magmatic intrusions, volcanism, deposition and erosion. Chillagoe Limestone Formation is approximately 450 million years old and is composed of reef debris and limey mud (Plimer, 1997). This limestone is one of the main lithologies that shape the present Chillagoe region. Cave formation in the Chillagoe limestone most likely began about 300 Ma but occurred extensively from 60-35 Ma and 24-6 Ma, during warm wet tropical conditions (Plimer, 1997). The limestone bluffs now consist of rugged limestone towers, with many large and small cavities, with and without decoration (Lees, 1899). The karstic limestone region of Chillagoe is enclosed by metamorphic rock in the southwest and granitic rock in the North and East (Lees, 1899; Willmott and Trezise, 1989).

Quincan Crater

Quincan Crater lies on the volcanic mountain Mt Quincan in the middle of the Atherton Tablelands close to the small town Yungaburra, Northeast Queensland, Australia. The crater at 17.3 °S 145.58°E is 800m in diameter and lies on the eastern side of Mt Quincan. In the middle of the crater lies a swamp 260 m in diameter, 790 m above sea level, with no in- or outflows (Kershaw, 1971). The crater lies 100 km westward of Chillagoe and is likely to be subject to a comparable tropical climate.

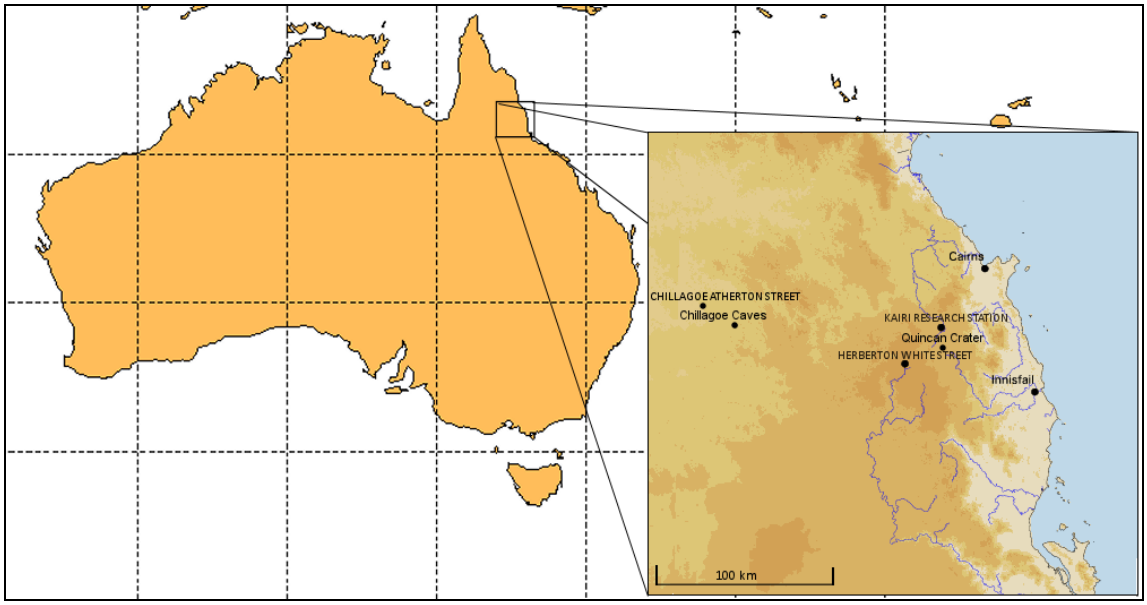

Figure 1: Location of the sample sites (Chillagoe Caves and Quincan Crater) and station sites (Chillagoe Atherton Street, Kairi Research Station and Herberton Post Office) in North Queensland, Australia. (BOM, 2010)

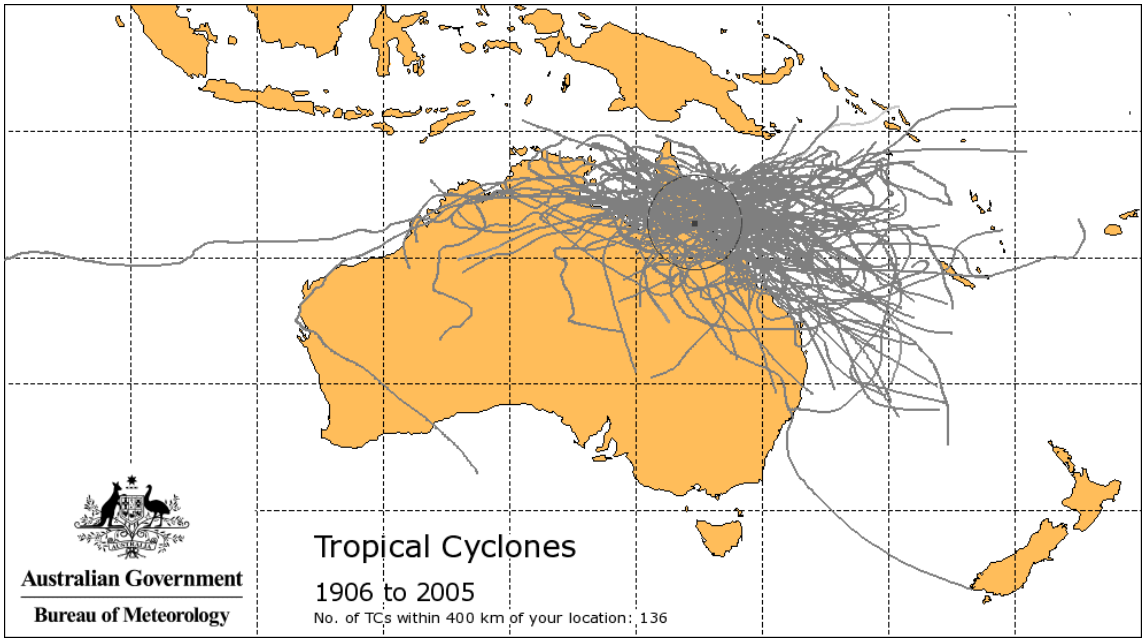

Figure 2: Tracks of Tropical Cyclones passing within 400 km of the Chillagoe Caves, North Queensland, Australia between 1906-2005 (BOM, 2010)

Material & Methods

Peat Core

Peat core Qui-1 was collected in 2003 from the edge of the swamp present in the Quincan crater using a CLAYMO manual peat corer. The 90 cm core was sectioned into 1 cm thick slices. The age model is based on analysis and calibration of Carbon-14 content of 12 samples. These samples came from 11 depths: 7-8 cm (one leaf sample, one bulk sample), 21-22, 30-31, 40-41, 44-45, 50-51, 60-61, 70-71 and 80-81 cm. The samples were sent to the Poznań Radiocarbon Laboratory, Poznan, Poland, where they were analyzed using accelerator mass spectrometry (AMS). The samples were calibrated using two methods: the Calibomb (samples younger than 1950) and the Oxcal program (samples older than 1950). The Calibomb program returns multiple possible calendar years based on the C-14 content of the samples, taking into account the influence of bomb testing. The Oxcal program gives a best fit age model based on the C-14 content and depth of the samples.

GDGT Analysis

Continental air temperature was reconstructed using the relative distribution of branched GDGTs content of the peat samples using the MBT/CBT method (Weijers et al., 2007). The GDGT's are arranged in 3 groups of 3, based on the amount of methyl branches (4, 5 or 6) and cyclopentyl moieties (0, 1 or 2) (see appendix 1) (Sinninghe Damsté et al., 2000; Weijers et al., 2006). Two ratios have been developed using these groups: the cyclisation ratio of branched tetraethers (CBT) and the methylation index of branched tetraethers (MBT) (Weijers et al., 2007).

In order to analyse the branched GDGT content the samples from 3-45 cm depth were ovendried at 40 °C for 3-4 days and ground. The ground samples were extracted using an Accelerated Solvent Extractor (ASE) with a dicholoromethane (DCM) and methanol (MeOH) mixture (9:1 v/v). Solvents were evaporated using a rotary evaporator and/or a nitrogen stream. Excess water was removed by sodium sulphate. Of each sample, 10mg was separated into a non-polar and polar fraction by aluminium oxide column chromatography using hexane and DCM as eluents respectively. The polar fraction was dissolved with hexane/isopropanol (99:1 v/v) to a 2mg/ml concentration and then filtered through a 0.4 µm PTFE filter.

GDGT content of the samples was analysed using a High Performance Liquid Chromatography/Atmospheric Pressure Chemical Ionisation-Mass Spectrometer (HPLC/APCI-MS) on an Agilent 1100 series machine equipped with automatic injector at the Royal Netherlands Institute

for Sea Research (NIOZ). The concentrations of GDGT isomers (see Appendix 1) were determined using the HP Chemstation software. Continental air temperature was reconstructed using the following three formulas (Weijers et al., 2007):

$$CBT = -\log\left(\frac{[1020]+[1034]}{[1022]+[1036]}\right) \quad (1)$$

$$MBT = \frac{[1022+1020+1018]}{[1022+1020+1018]+[1036+1034+1032]+[1050+1048+1046]} \quad (2)$$

$$MBT = 0.122 + 0.187 * CBT + 0.020 * MAT \quad (3)$$

The reconstructed air temperature was compared to temperature data from the weather stations Herberton White Street (No. 031029) 26.8 km from the core site and Kairi Research Station (No. 031034), 3.8 from the core site (see Figure 1).

Stalagmite

The stalagmite CH2 was collected from a Chillagoe Cave (17.2°S, 144.6°E) in May/June 2006. It was actively dripping when collected indicating growth at the time of collection. The stalagmite was sectioned vertically along its growth axis showing an uninterrupted growth history of alternating ochre and white calcite layers. A 1 cm thick section was prepared from one half, embedded in resin, polished and cleaned with OHQ water in an ultrasonic bath.

The chronology of the stalagmite is based on seasonal layer deposition and layer thickness. A white calcite layer is deposited during the dry season and a dark, organic matter rich layer during the wet season. By counting these layers a reliable chronology is constructed. In addition, layer thickness was compared to precipitation data from Chillagoe Atherton Street (station no. 030140, 9.9 km away from the cave (Figure 1)) to identify any lags in the dataset. This method is based on the observation that a higher amount of rain leads to thicker layers (Betancourt et al., 2002; Brook et al., 1999; Rasbury and Aharon, 2006). The layer counting and thickness measurements were performed on a scanned image of the stalagmite at a resolution of 9600 dpi.

Isotope Analysis

The first 1.5 cm of the stalagmite section was sub-sampled at a seasonal resolution using a video-controlled micromill with 40x optical zoom. To perform the Hendy Test for isotopic equilibrium, 3 samples were collected along a single light calcite layer. Measured along the growth axis, this layer occurs 18.4 mm from the apex. The samples were collected using a scalpel and brush, which were cleaned with ethanol between samples. The stalagmite was cleaned using compressed Argon or Nitrogen gas between samples. The first two layers were not sampled as they were too close to the edge to sample properly. The sub-sampling corresponds to 210 seasonal layers (105 years) of active growth covering the instrumental climate record for the Chillagoe region.

Oxygen and carbon isotope analysis was performed on the 210 calcite samples of 35-45 µg using a Kiel III carbonate device coupled to a Finnigan MAT 253 IRMS. The calcite samples were reacted with 3 drops of H_3PO_4 at 70 °C. Using the standard NBS-19 with a known isotopic composition of $\delta^{18}O$: -2.20‰vPDB and $\delta^{13}C$: 1.95‰vPDB with a standard deviation of 0.04‰ for $\delta^{13}C$ and 0.06‰ for $\delta^{18}O$, the data for each run were normalized. All measurements are reported relative to Vienna PeeDee Belemnite (vPDB) by using the standard NBS-19 and reference gas.

Wavelet Analysis

Wavelet analysis was performed on the Southern Oscillation Index (SOI), Interdecadal Pacific Oscillation (IPO), SST of the Niño-4 area (5°S-5°N; 160°E-150°W), layer thickness, $\delta^{18}O$ and $\delta^{13}C$ record. SOI data were provided by the Australian Bureau of Meteorology (BOM, 2010). The IPO data, last updated in 2005, were provided by the Hadley Centre, UK. The Global Climate Observing System provided the sea surface temperatures (GCOS, 2009). The analysis was performed online using a Morlet Wavelet (Torrence and Compo, 1998). The wavelet analyses were compared to determine if any similarities in periods are present.

Instrumental Climate Data

Historical climate data shows gaps and is prone to artificial trends. These gaps and trends are caused by several non-climatic influences on climate data. Nicholls et al (2006) present a general list consisting of changes in site location, local environment (e.g. urbanization), network distribution, instrumentation and observing practices. Interpretations of climate databases must always be handled with care (Nicholls et al., 2006). Table 3 shows an overview of the temporal limitations per weather station. Due to the fact that no automated weather station has been installed at Chillagoe, rainfall observations are taken by volunteers. In some exceptional cases when no volunteers were

present, no measurement could be made and the precipitation amount on the next day will be the sum of two days.

Table 1: Data availability for the Weather Stations in the study area

Weather Station	Precipitation	Temperature
Chillagoe Atheron Street	1902-2010	-
Kairi Research Station	-	1953-2010
Herberton White Street	-	1907-1990

Tropical Cyclone Dataset

The Australian tropical cyclone best-track dataset was revised in 2008 in order to improve its reliability. Artifical trends are present due to an increased number and more detailed observations per day and more accurate techniques (Trewin, 2008). Observation techniques have become increasingly accurate since the introduction of radar data in 1954, prior to this all cyclone reports were generated from surface observations (Trewin, 2008). The number and accuracy of tropical cyclone observations increased in 1972 with the development of the Dvorak technique, which uses satellite images (Kuleshov et al., 2010; Landsea et al., 2006; Trewin, 2008). In 1984, the Dvorak technique was improved with the introduction of infrared methods. Prior to this, tropical cyclone central pressure is usually underestimated (Landsea et al., 2006; Trewin, 2008).

Results

The results from the stalagmite and peat core analyses are described below. For the stalagmite, these results are the outcome of the Hendy test, a reliable age model and a reconstructed $\delta^{18}O$ depletion record. An age model and reconstructed mean air temperature have been composed for the peat core.

Peat Core Age Model

Figure 3 shows the age model based on 12 ^{14}C-dates taken from the Quincan Crater Sediment Core (Qui-1). The model exists of two separate calibration curves which overlap between 40-45 cm depth indicating a good fit. Both calibration curves correlate well with all the ^{14}C-dated samples (R^2=0.998). Two samples at 21.5 and 30.5 cm depth have not been used for the calibration due to the high uncertainty (± 156.5 years) associated with these two points. The age model shows a gentle slope at the top of the core, which increases toward 80 cm depth. This indicates an apparent higher sedimentation rate in the past, most likely due to compaction.

Mean Air Temperature

Figure 4 shows the mean temperature curve as generated from the GDGT content of the Quincan Core (Qui-1). The reconstructed temperature curve is stable, with temperatures ranging between 21°C and 28°C. Temperatures remain steady around 27°C between 1778-1904, whilst a general cooling trend is present between 1925-1994. Significant oscillations in the temperature curve occur from 1904 to 1925 where temperatures range from 24.8°C to 27.8°C. Exceptions on the general cooling trend include a short warming trend between 1940-1949, and two warm years in 1965 and 1997.

Stalagmite Age Model

An age model for CH2 has been established based on layer counting. To verify the age model and identify any lags, measured thickness of 210 seasonal growth layers of the Chillagoe stalagmite (CH2) (105 dark and 105 light layers) and seasonal instrumental rainfall data (wet and dry season) over the last 100 years were compared (Figure 5). The layer thickness record corresponds well to the instrumental rainfall record in that both follow the same general pattern over time. In most cases a peak in layer thickness corresponds to a peak in precipitation, while approximately half of the peaks in precipitation have a corresponding peak in layer thickness. A similar relationship is observed between troughs in the layer thickness record and the precipitation record. All peaks in layer thickness which correspond to a peak in precipitation are dark layers (60 peaks). Exceptions to this include 9 peaks in layer thickness which do not correspond to a peak in precipitation, all of which are

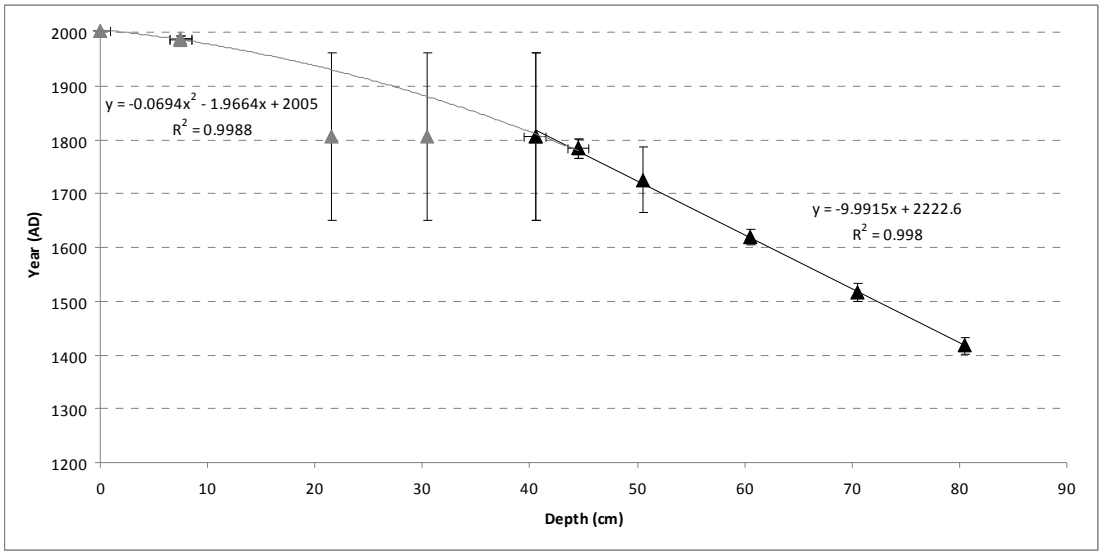

Figure 3: Age model of Qui-1 based on ^{14}C- dating, Quincan Crater, North Queensland, Australia, between 1417-2003.

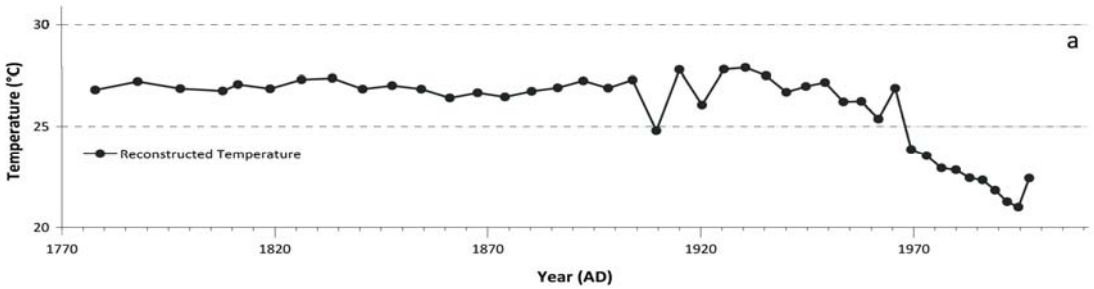

Figure 4: Reconstructed Mean Temperature (MT) between 1778-1997 generated from a core sampled from Quincan Crater, North Queensland, Australia.

light coloured layers. A strong correlation between peaks occurs above a precipitation amount of 1000 mm in which 15 out of 19 precipitation peaks correspond to a peak in layer thickness. The best match occurs between 1914-1916, 1936-1942, 1947-1960 and 1976-1978, whilst covariance is poor between 1929-1934, 1960-1967 and 1979-1990. The covariance between these two records indicates that in most cases a high precipitation amount leads to the deposition of a thick layer. This is in agreement with previous studies (Betancourt et al., 2002; Brook et al., 1999; Rasbury and Aharon, 2006).

Given the amount of noise present in Figure 5, the rainfall and layer thickness datasets were smoothed by calculating the 2.5 years floating averages in order to decipher any long-term periodicities (see Figure 6). These smoothed records still correlate well with respect to general trends, however oscillations in these curves do not occur simultaneously. The instrumental precipitation curve still exhibits significant seasonal variability while this detail is lost in the layer thickness curve, indicating a lesser seasonal influence on the layer thickness. The layer thickness curve lags 1-3 years behind the precipitation curve. This lag is most prominent between 1940-2007, particularly between 1948-1952, 1954-1957, 1973-1976 and 1987-1990. These periods also clearly show the variability of the lag with time. The two records do not match as well between 1902-1940, where layer thickness increases, while precipitation remains relatively stable.

Figure 7 shows the relationship between layer thickness and corresponding precipitation between 1902-2005. The majority of the layers within CH2 are between 40-60 µm thick while 19 % is thicker than 80 µm. These thicker layers correspond, for 50 %, to above average wet season precipitation amounts (i.e. above 780 mm). Only 5 of these thicker layers are light layers and correspond to dry season precipitation. Majority of the data points below 80 µm in thickness correspond to precipitation below 780 mm. However, a number of exceptions occur which may indicate that a threshold of 400 mm needs to be reached over time in order for these thicker layers to form. Instances where thick layers correspond to low precipitation amounts occur in the dry season of 1932, 1935, 1960, 1962, 1984 and in the wet season of 1976-1977. Similarly exceptions exist where thin layers correspond to high precipitation amounts, particularly in 1903, 1950, 1955, 1973, 1975.

Isotope analysis

Hendy Test for Equilibrium

Figure 8 shows the results of the Hendy test of CH2 in a scatter plot of the $\delta^{18}O$ and $\delta^{13}C$ values of three samples along a light calcite layer 18.4 mm from the apex. The first sample was taken 3.66 mm

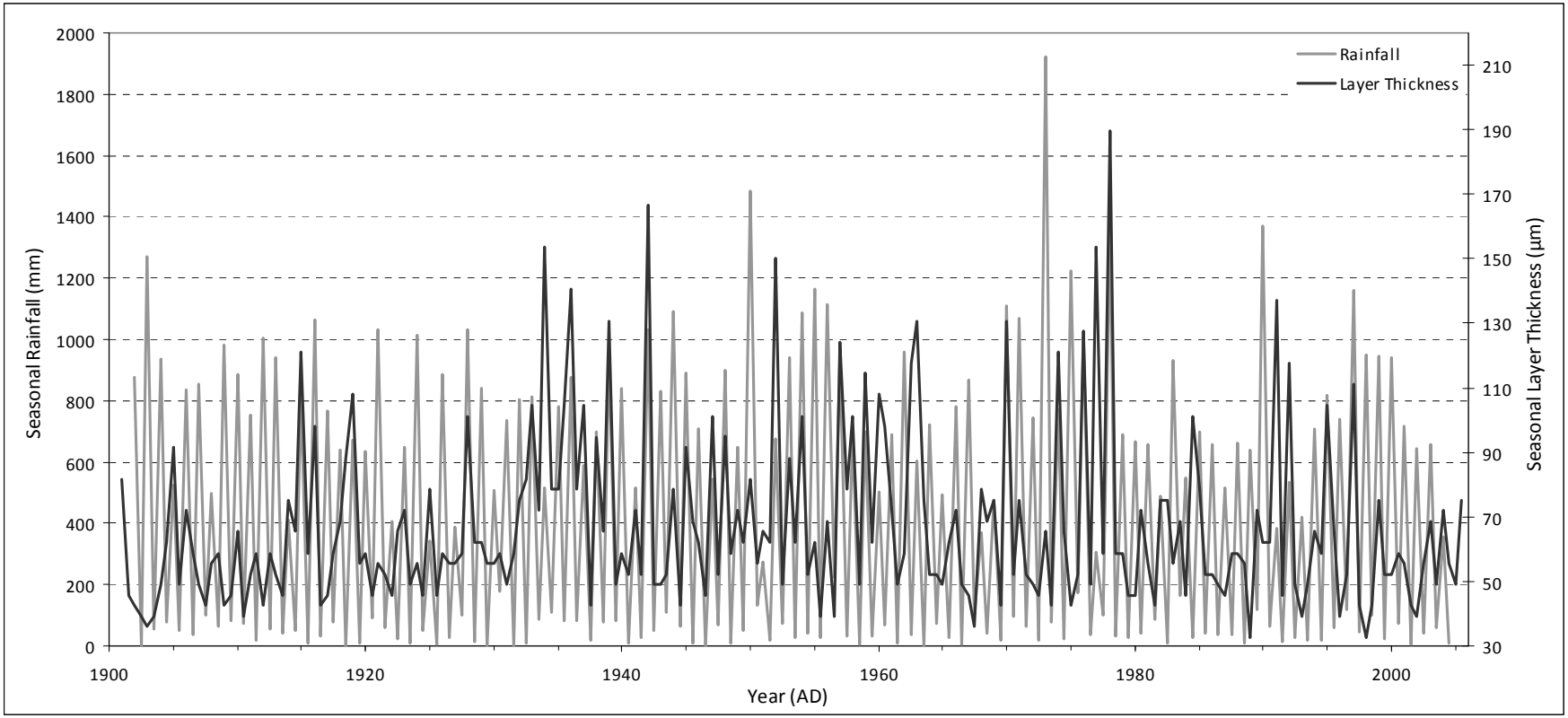

Figure 5: Comparison between layer thickness of CH2 (dark and light layers) and instrumental seasonal rainfall (wet and dry season) from 1902-2005.

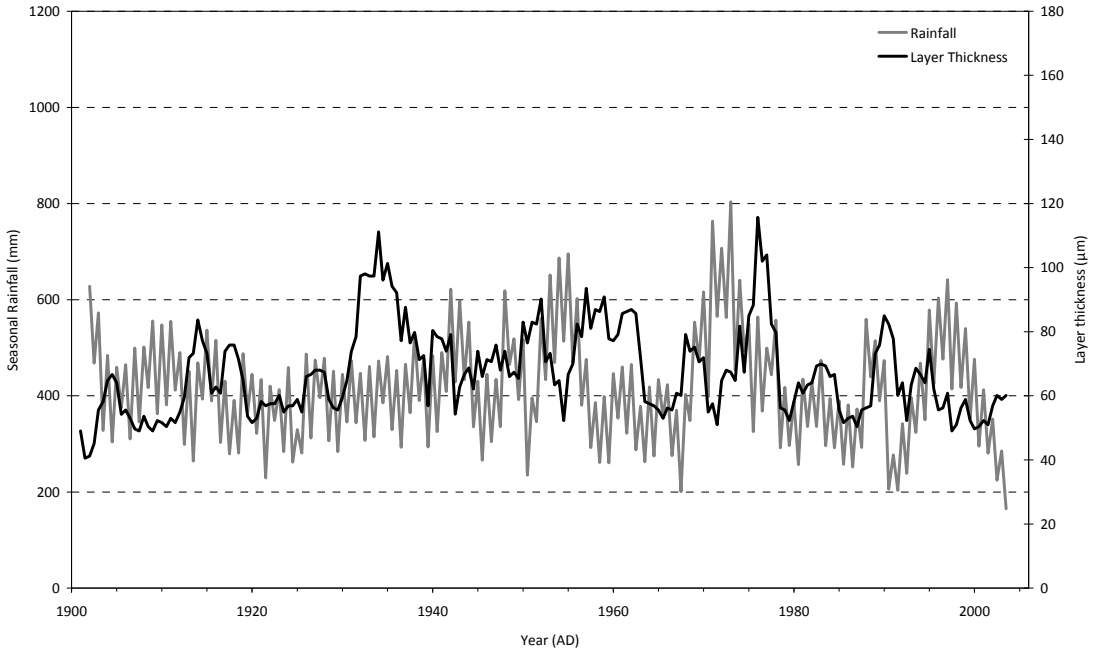

Figure 6: Comparison between stalagmite layer thickness (dark and light layers) and instrumental seasonal rainfall (wet and dry season) from 1902-2005. (Note: 2.5-yr moving average has been applied to both datasets).

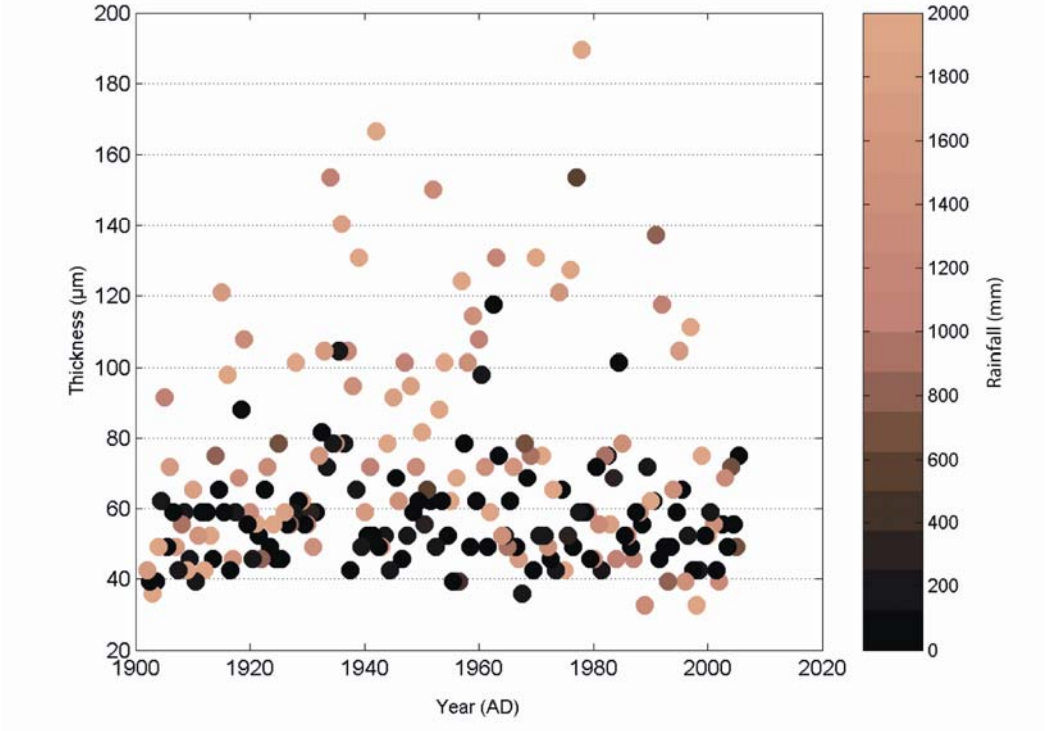

Figure 7: 3D scatter plot showing the relationship between precipitation amount and corresponding stalagmite growth over time.

right of the growth axis, while the second and third sample were taken 3.92 and 10.33 mm left of the growth axis respectively. The layers vary in thickness: 61.25 µm at the first sample location and 87 µm and 56.95 µm for sample 2 and 3 respectively. The two samples with the thinnest layer thickness are more depleted in ^{18}O compared to the thicker sample. The maximum difference between the $\delta^{18}O$ values is 0.584 ‰, for $\delta^{13}C$ this is 0.293 ‰.

The correlation between $\delta^{18}O$ and $\delta^{13}C$ values from CH2 is shown in Figure 9. A linear trendline of all the $\delta^{18}O$ and $\delta^{13}C$ data, from 1901-2005, (short dotted line) reveals a positive relationship with an R^2 of 0.455. Splitting the dataset into two shorter datasets, 1901-1983 and 1983-2005, leads to strong positive linear correlations. Strong correlations in 1901-1983 (R^2 0.76) and 1983-2005 (R^2 0.86) indicate a covariance of $\delta^{18}O$ and $\delta^{13}C$ in CH2 which strengthened around 1983.

$\delta^{18}O$ record

Figure 10 shows the $\delta^{18}O$ depletion curve generated from the most recent 210 seasonal growth layers of CH2. The $\delta^{18}O$ depletion curve is highly variable, ranging between -1.6‰ and -7.5‰. Major oscillations occur between -4‰ and -6‰ with a general trend toward more positive values in 2005. The majority of $\delta^{18}O$ minima and maxima correspond to wet season growth, whilst the majority of dry season values lie in between. The three-year moving average applied to the dataset indicates a phase change approximately every 10-25 years. More significant negative phases in the isotope record occur between 1910-1926 (~ -7.5‰) and 1941-1956 (~ -7.2‰) while a more positive phase occurs between 1977-1982 (~ -1.6‰). Within these phases, smaller scale oscillations occur with a periodicity of approximately 1-5 years, the majority of which have a periodicity of 2 years. An abrupt positive excursion occurs between 1970 and 1981 followed by a return to more negative values between 1981 and 2005. During this period, the annual variability in $\delta^{18}O$ increases significantly, exhibiting an amplitude shift of 1‰ - 2‰ in some cases.

A comparison between the wet and dry season $\delta^{18}O$ curves (see Figure 11) shows two very similar records. While both curves generally exhibit the same trends through time, the corresponding wet and dry season $\delta^{18}O$ values are not identical. This offset between the two seasons is not constant and varies between +1‰ and -1‰. More variability in the seasonal offset occurs between 1968-2005, with extremes of -2.27‰ (1982) and +1.5‰ (1997). The period of greater variability between 1981-2005 is due to large annual variations in wet season $\delta^{18}O$ as noted previously from Figure 9. The corresponding dry season $\delta^{18}O$ values appear to be an average of these extremes.

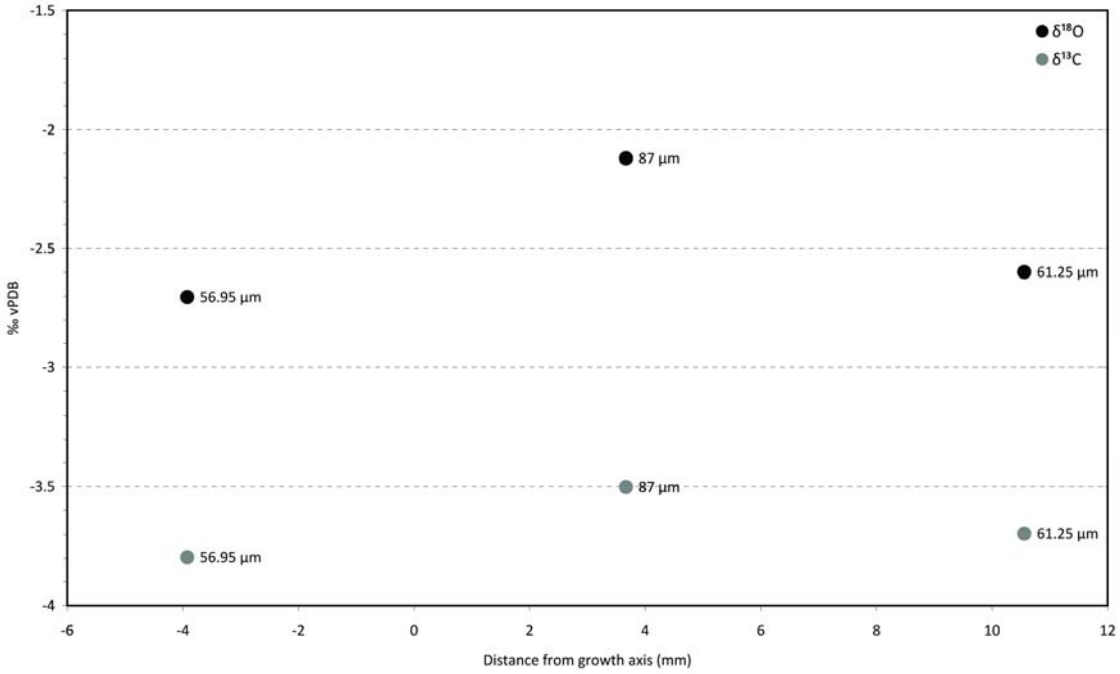

Figure 8: $\delta^{18}O$(black) and $\delta^{13}C$(grey) values of 3 samples along a light calcite layer of stalagmite CH2 (note: data labels show average layer thickness at sample location)

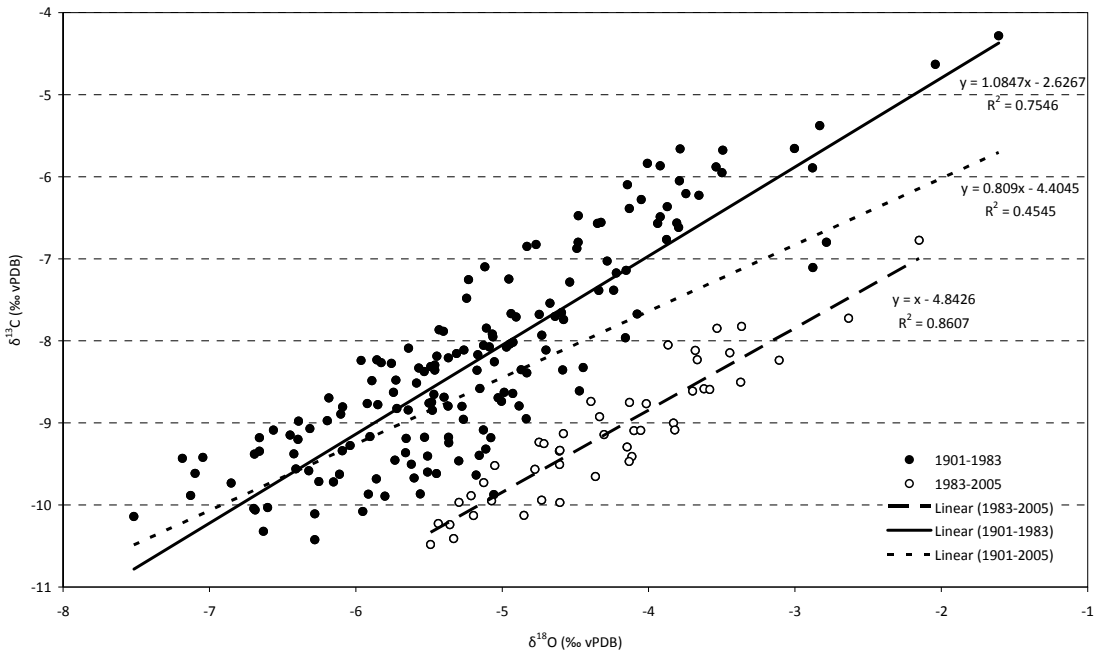

Figure 9: Scatter plot of $\delta^{18}O$ versus $\delta^{13}C$ of stalagmite CH2 (‰ vPDB) between 1901-2005 (all circles, short-dotted trendline), 1901-1983 (black circles, black trendline) and 1983-2005 (open circles, long dotted trendline)

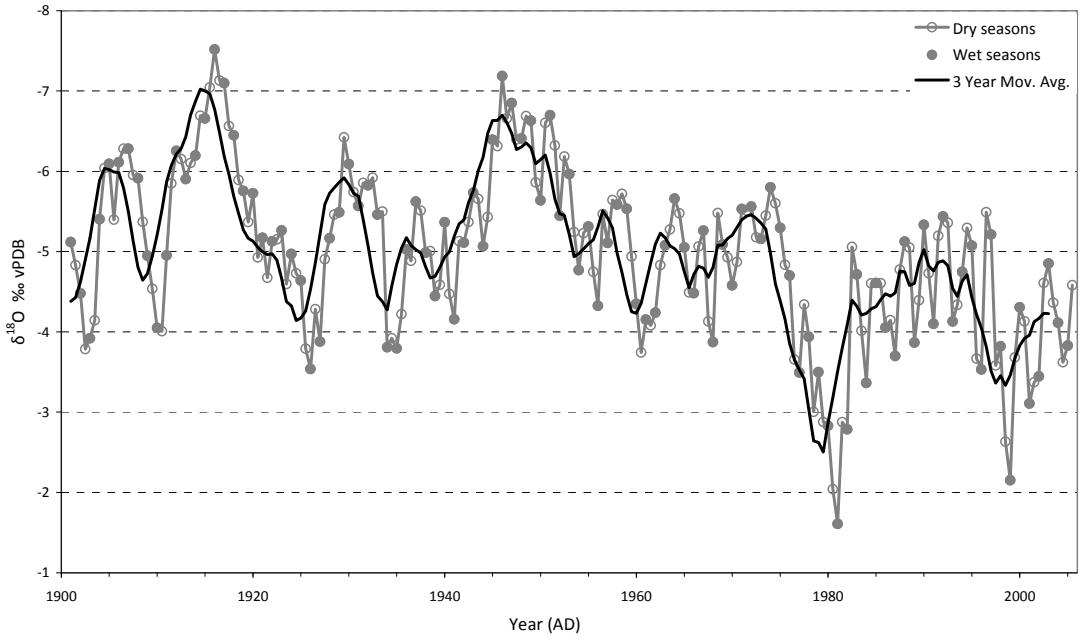

Figure 10: Seasonal $\delta^{18}O$ depletion curve (‰ vPDB) generated from CH2, Australia between 1901-2005 (dry season data: open circle; wet season data: filled circle; trendline: 3-yr moving average).

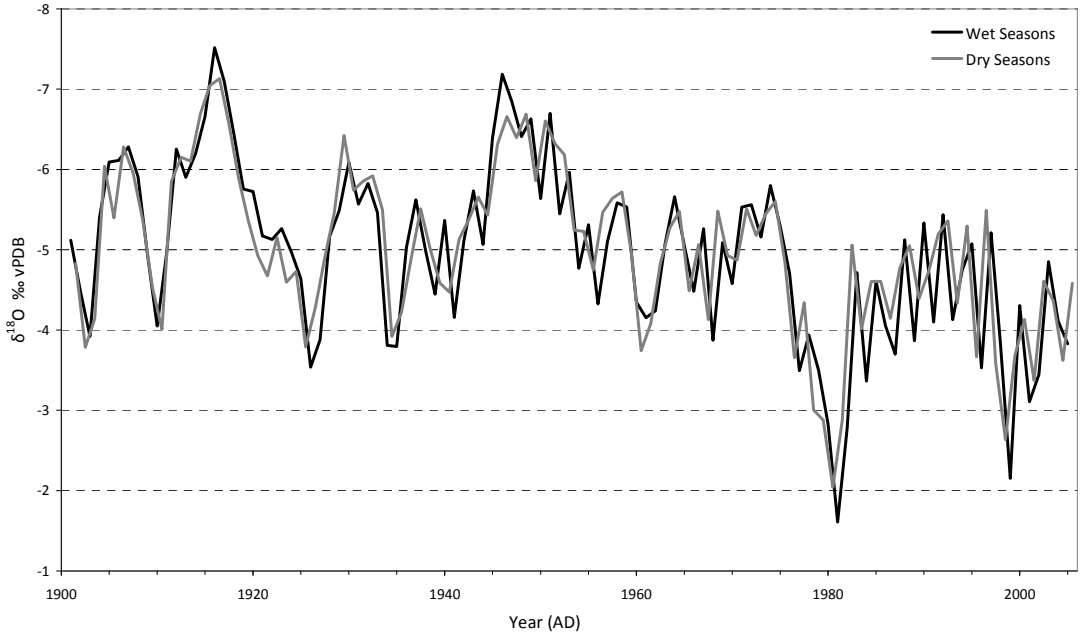

Figure 11: Comparison between wet season (black curve) and dry season (grey curve) $\delta^{18}O$ values (‰ vPDB) generated from CH2, between 1901-2005.

Discussion

Peat core Qui-1 was analyzed for its use in paleoclimate reconstructions. A reliable age model has been developed for this record. Figure 12a shows the comparison between the reconstructed temperature curve and instrumental mean maximum annual temperatures measured by two weather stations in North Queensland (3.8 km and 26.8 km from the study site respectively). Figure 12b shows a similar comparison with instrumental mean maximum summer temperatures. The instrumental records show similar stable curves with small oscillations. The reconstructed temperature curve matches well with both instrumental records in terms of the overall trend, however exhibits a closer match to the summer record with respect to absolute temperature values. The instrumental summer temperature record and the reconstructed temperature record correlate reasonably well from 1907–1949. They both show the oscillations noted previously between 1904-1925, the onset of a cooling trend in 1925 and the small warming trend between 1940-1949. However, the records deviate after 1949. The instrumental summer temperature record remains relatively constant between 1949-2010, whilst the reconstructed temperature record shows a cooling trend.

Air temperatures reconstructed from Qui-1 coincide with the changes in instrumental summer temperatures, indicating the peat core accurately records the regional climate. These findings are consistent with other studies (Peterse et al., 2009a; Peterse et al., 2009b; Sinninghe Damsté et al., 2008). As noted above, the records begin to deviate after 1949, indicating a change in local environment without a corresponding change in regional climate. This change in proxy usability may be caused by both natural and anthropogenic influences. Several identified human activities include damming of the Barron River (1953-1958) to create Lake Tinaroo (10 km North of Mount Quincan) and the development of the Mareeba-Dimbulah Irrigation Area (1955) (EPA, 2002). Exactly how any of these activities, if any, would influence usability of the proxy is not known. It is not yet fully understood what bacteria are responsible for the production of branched GDGT's nor is their distribution in the soil or the impact of decay. Nevertheless, the observed deviation indicates the top 17 cm of this peat core may be less useful for reconstructions.

Stalagmite CH2 was analyzed for its ability to accurately record tropical cyclones passing within 450 km of Chillagoe. The comparison between layer thickness and instrumental rainfall data indicated a 1-3 year lag in the age model of CH2; such a lag is also seen in other studies in tropical stalagmites and appears to be caused by a complex stalagmite feeding system containing many fissures and a possible water reservoir (Brook et al., 1999; Rasbury and Aharon, 2006). The lag may also be caused

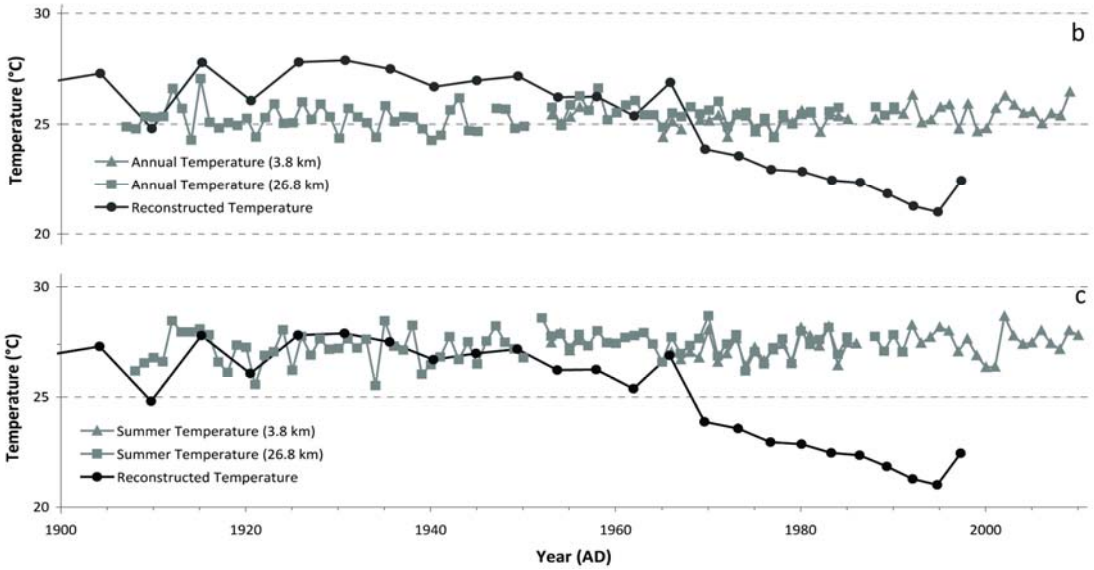

Figure 12: a) Comparison between the reconstructed MT and instrumental mean maximum annual temperatures from the two closest stations; Kairi Research Station (data available from 1953-2010) and Herberton White St (data available from 1907-1990). b) Comparison between the reconstructed MT and instrumental mean maximum summer temperatures from the same two stations presented in a).

by a shift in the age model caused by missing layers. An extremely dry year could result in no calcite being deposited. Analysis of trace elements in CH2 may determine the exact water residence time, as they are known to be related to precipitation amount, productivity and the groundwater pathway (Fairchild et al., 2000; Fairchild and Treble, 2009; Treble et al., 2003; Treble et al., 2005b).
As described above the dry and wet season $\delta^{18}O$ depletion curve are nearly identical. This similarity indicates the data set possibly shows an annual signal rather than a seasonal signal. This annual signal could be caused by a combination of sampling limitations and mixing in a water reservoir between seasons. The combination of this annual signal and the lag in the age model diminishes the use of CH2 to identify individual tropical cyclones.

Kinetic isotopic fractionation will lead to simultaneous enrichment of ^{18}O and ^{13}C in a stalagmite as well as more heavy isotope enrichment towards the edges of the stalagmite (Hendy, 1971). With a maximum difference of 0.584 ‰ in $\delta^{18}O$ along a single calcite layer, CH2 passes the first criterion of the Hendy test (e.g. <0.8‰ difference along a single layer) (Hendy, 1971). However, the second criterion is not met due to covariance of the $\delta^{18}O$ and $\delta^{13}C$ records (Hendy, 1971). Though the Hendy Criteria are widely used, an increasing number of studies indicate that $\delta^{18}O$ and $\delta^{13}C$ covariance does not necessarily imply kinetic fractionation and alternative methods to exclude kinetic fractionation have been suggested such as replication (Dorale et al., 1998; Dorale et al., 1992; Dorale and Liu, 2009; Genty et al., 2006; Griffiths et al., 2010; McDermott, 2004; Treble et al., 2005a). Moreover, the Hendy test assumes no climate-driven changes in $\delta^{13}C$, however many studies have indicated $\delta^{13}C$ is often influenced by environmental factors such as precipitation and vegetation type (C3 and C4 plants have distinct different $\delta^{13}C$ values). A high amount of precipitation will lead to more production of the vegetation, taking up more ^{12}C from the surrounding soil. This leaves the soil enriched in ^{13}C which is subsequently transferred to the groundwater and eventually incorporated in the stalagmite. (Denniston et al., 1999; Dorale et al., 1998; Dorale et al., 1992; Frappier et al., 2002; Genty et al., 2001; Hellstrom et al., 1998; Linge et al., 2001; Verheyden et al., 2008).

Multiple environmental factors have been found to influence ^{18}O in stalagmites. Previous studies have often linked $\delta^{18}O$ to precipitation amount, where a higher amount of precipitation leads to more ^{18}O depletion (Fleitmann et al., 2004; Frappier et al., 2007; Hellstrom et al., 1998; McDermott, 2004; Nott et al., 2007; Treble et al., 2005a; Treble et al., 2007; Verheyden et al., 2008). Figure 13a shows the comparison between the $\delta^{18}O$ depletion curve from CH2 and instrumental seasonal rainfall data from Chillagoe Atherton Street Station The precipitation and $\delta^{18}O$ depletion curve (see Figure 13a) show no apparent correlation. The seasonal rainfall curve shows mainly seasonal oscillations, whilst the $\delta^{18}O$ depletion curve mainly shows oscillations with a period of 1-5 years. The

two curves also differ in amplitude. Large changes in precipitation amount do not correspond to large changes in $\delta^{18}O$ and vice versa. The differences are most obvious between 1910-1926, 1941-1956 and 1977-1982. The absence of correlation between high amounts of rainfall and low $\delta^{18}O$ values indicates $\delta^{18}O$ changes in CH2 can not be explained by amount effect.

Former studies have also linked $\delta^{18}O$ to temperature changes (Denniston et al., 1999; Dorale et al., 1998; Dorale et al., 1992; Goede, 1994; Lauritzen and Lundberg, 1999; Linge et al., 2001; Spötl et al., 2002; Thompson et al., 1976). Figure 13b shows the comparison between the $\delta^{18}O$ depletion curve from CH2 and the mean seasonal maximum temperature record from Herberton White Street Station. The $\delta^{18}O$ depletion curve is very different from the seasonal mean maximum temperature. The long term (10-24 years) variations in the $\delta^{18}O$ depletion curve are not seen in the temperature curve. On the other hand, the seasonal variations in mean maximum temperature show no correlation to the $\delta^{18}O$ depletion curve. If temperature alone would influence the $\delta^{18}O$ curve, the range in $\delta^{18}O$ (-1.6‰ to -7.5‰) would indicate a change in temperature from 18 to 5°C respectively. Neither such a change in temperature nor the absolute values are seen in Figure 13b indicating temperature is not the driving force for $\delta^{18}O$ changes in CH2.

As discussed above, kinetic fractionation, temperature and precipitation amount are excluded as the main influence on the $\delta^{18}O$ record. Consequently the only influence on the $\delta^{18}O$ depletion record is the isotopic composition of precipitation, which in turn is extensively affected by tropical cyclone activity. Table 2 shows an overview of all cyclones passing within 450km of the Chillagoe Caves between 1907-2008 in 50 km increments. In total, 149 tropical cyclones passed within 450 km of the site. As discussed before, the dataset is most reliable between 1955-2006, therefore we focus mainly on the tropical cyclone data in this period. Between 1955 -2006, 87 tropical cyclones passed within the 450 km study area.

Table 2: Overview of the number of tropical cyclones passing within range (0-450 km) from the Chillagoe Caves from 1907-2008

Year	0-50	0-100	0-150	0-200	0-250	0-300	0-350	0-400	0-450
1907-2008	5	20	37	55	77	90	110	132	149
1955-2008	3	12	20	31	42	51	64	77	87

In Figure 14, the frequency and category of tropical cyclones passing within 450 km have been plotted per year. The figure shows a slight increase in the number and strength of tropical cyclones from 1907 to 2008. Most of the tropical cyclones are a category 1 cyclone (i.e. above 985 hPa central pressure (see table 3)). The most intense tropical cyclones within this study area are category 4 (i.e. 920-945 hPa central pressure) and occured in 1918, 1991, 2005 and 2006. The highest frequency within 450 km of Chillagoe is 4 tropical cyclones per year (between 1907-2008), as was the case in

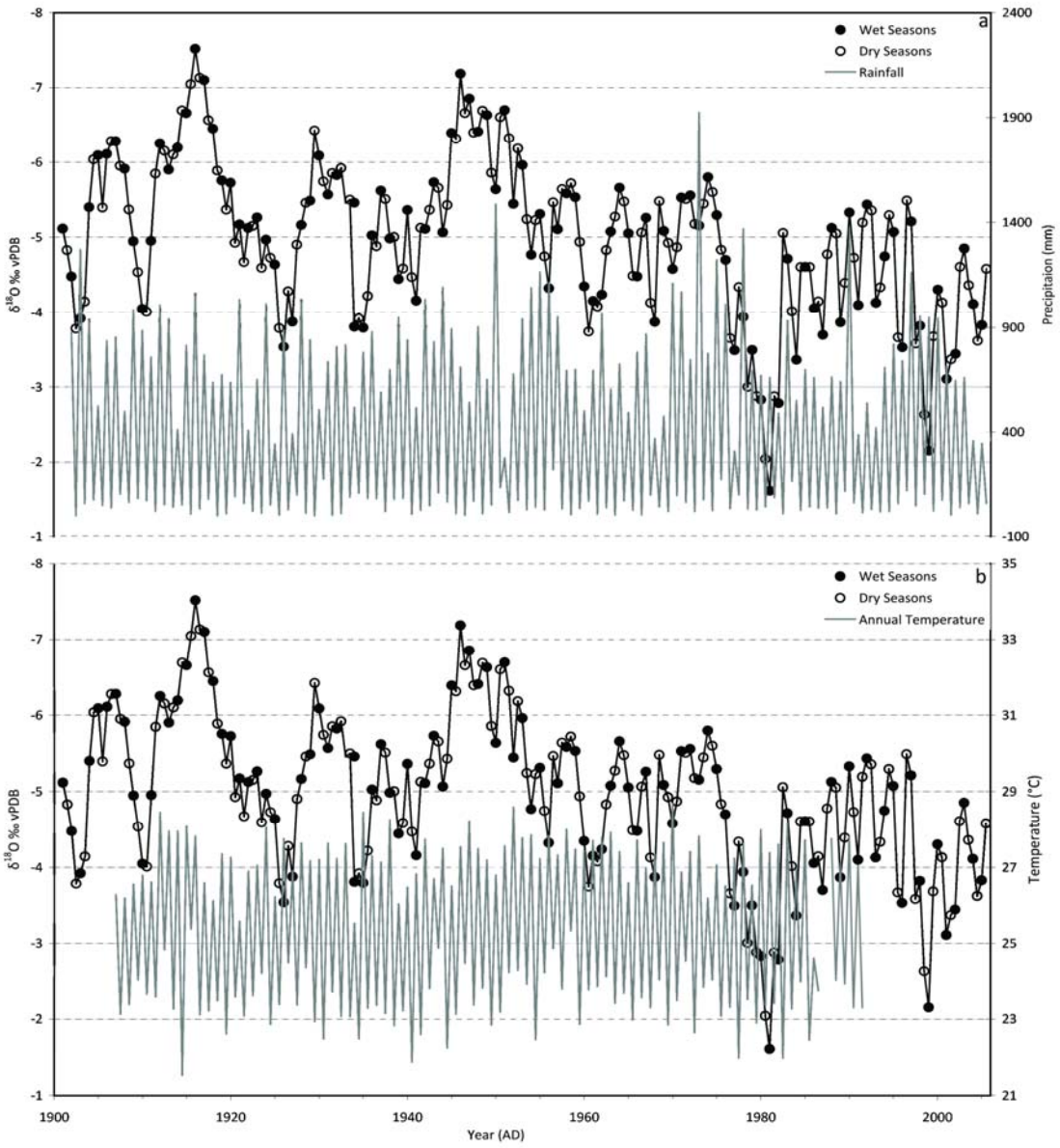

Figure 13: Comparison between the seasonal $\delta^{18}O$ depletion curve (‰ vPDB) and a) instrumental seasonal rainfall from the closest weather station (Chillagoe Atherton Street) between 1901-2005. b) instrumental seasonal mean maximum temperature from Herberon White Street weather station between 1907-1990.

1911, 1934, 1940, 1976, 1977, 1979 and 1985. In only 2 of these 7 high-frequency years has a tropical cyclone exceeded category 2. On the other hand, within this study area, category 4 tropical cyclones only occur in years with 2 cyclones per year or less between 1907-2006. Table 4 shows the total number of tropical cyclones per category within the study area between 1955-2005 and confirms that low intensity tropical cyclones occur more frequent than high intensity tropical cyclones.

Table 3: Category of tropical cyclones based on central pressure

Category	Central Pressure (hPa)
1	>985
2	970-985
3	945-970
4	920-945
5	<920

Table 4: Total number of tropical cyclones passing within 450 km of the Chillagoe Cave between 1955-2005, sorted by category

Category	Tropical cyclones
1	56
2	18
3	8
4	3
5	0

A comparison between the wet season $\delta^{18}O$ depletion curve and the frequency of tropical cyclones passing within 450 km of Chillagoe between 1955-2005 is shown in Figure 15. The two records show strong similarity in general trend. Both curves show long-term oscillations, with peaks between 1970-1987 and 1995-2003. The tropical cyclone frequency record increases first in both cases, followed shortly after by the $\delta^{18}O$ depletion curve. When considering the 1-3 year lag noted previously, a good correlation exists between tropical cyclone frequency within 450 km of the sample site and the $\delta^{18}O$ depletion within the stalagmite.

The value of $\delta^{18}O$ for precipitation becomes more negative with increasing tropical cyclone intensity and longevity and from the outer wall towards the eye (Lawrence and Gedzelman, 1996; Lawrence et al., 1998). The less frequent occurrence and the more negative $\delta^{18}O$ values of intense cyclones combined could explain the correlation between $\delta^{18}O$ and tropical cyclone frequency. A higher amount of weak tropical cyclones per year will lead to less $\delta^{18}O$ depletion compared to a lower amount of strong tropical cyclones per year. Tropical cyclone frequency only explains part of the $\delta^{18}O$ fluctuations, other influences may include tropical cyclone central pressure, distance to the cave and longevity before entering the study area as all of these factors affect the isotopic value of precipitation (Lawrence and Gedzelman, 1996; Lawrence et al., 1998).

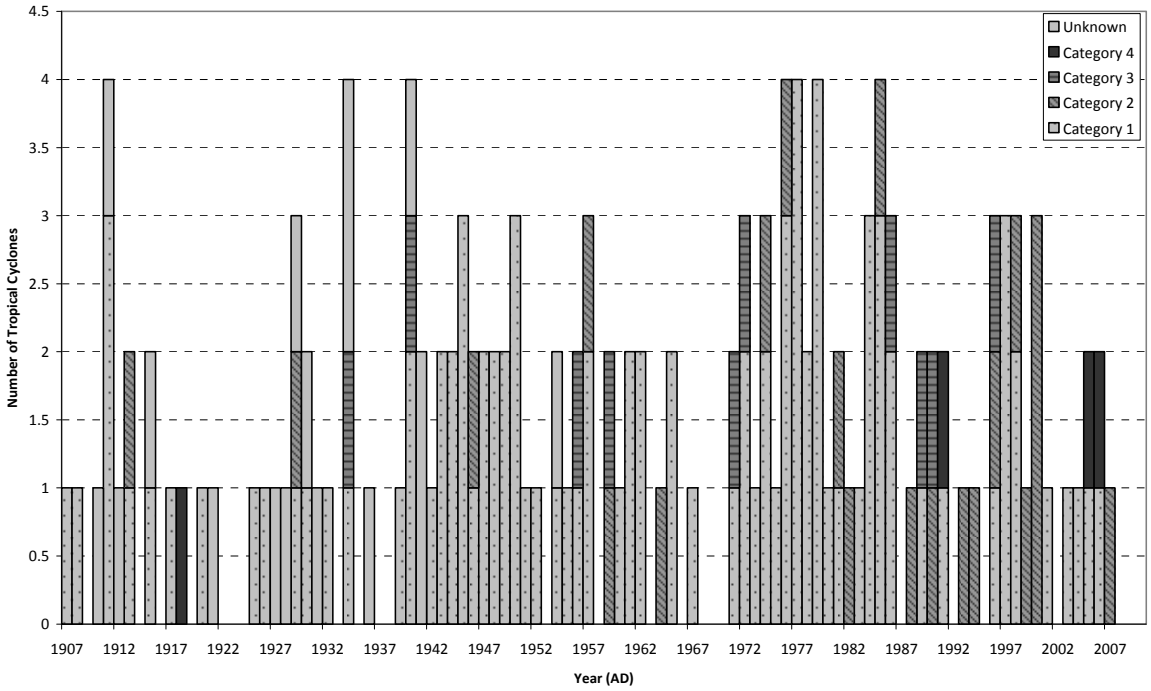

Figure 14: Number and category of tropical cyclones each year passing within 450 km of the Chillagoe Caves between 1907-2008

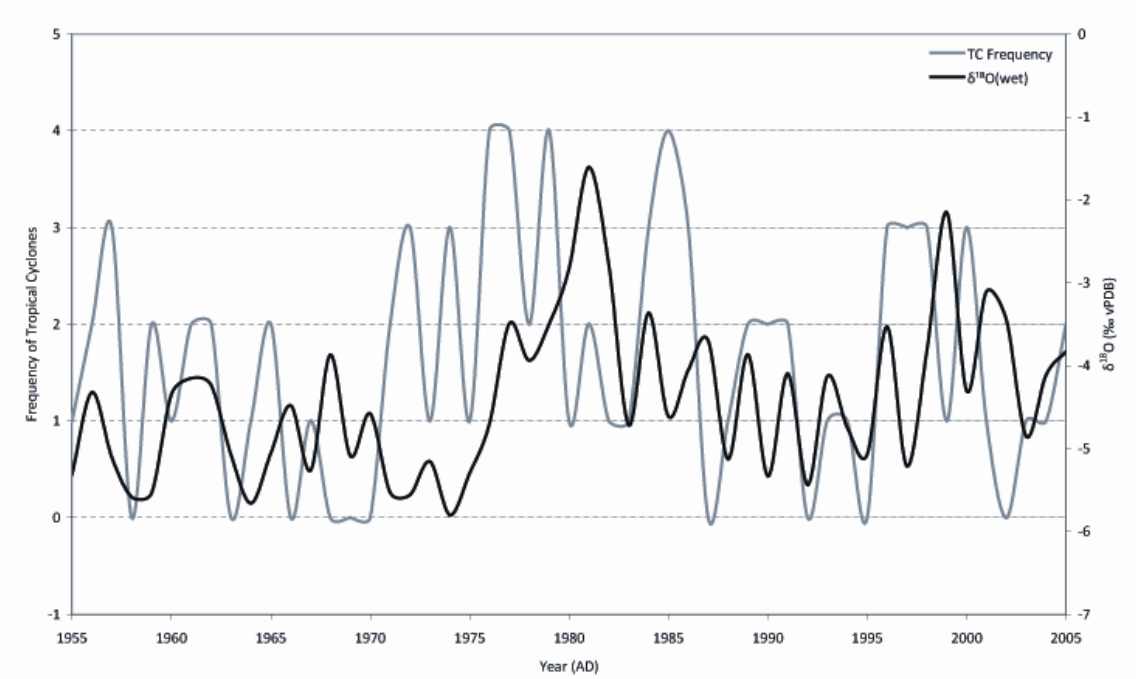

Figure 15: Comparison between the wet season $\delta^{18}O$ depletion curve (‰ vPDB) from CH2 and the number of tropical cyclones each year passing within 450 km of the Chillagoe Caves between 1955-2005.

Relationships between SST, SOI, IPO and the isotopic record are to be expected due to the SST dependence of tropical cyclone formation and its relationships with SOI (Allan, 1988; Chan, 1985; Fan and Liu, 2008; Holland, 1997; Nicholls, 1979; Ramsay et al., 2008). The Southern Oscillation Index is the air pressure difference between Tahiti and Darwin. A negative SOI coincides with an El Niño year (ENSO warm phase) and colder SST temperatures around Australia and the Niño-4 area.
Figure 16 and 17 show the results of wavelet analysis on the $\delta^{18}O$ and $\delta^{13}C$ depletion record, layer thickness, SST (Niño-4 area), Southern Oscillation Index (SOI) and Interdecadal Pacific Oscillation (IPO). Wavelet analysis does not pick up any strong spectra for the $\delta^{18}O$ record and layer thickness (16a,c). Nevertheless, the main period for the oxygen isotope record lies between 10-50 years, whilst for the layer thickness this lies between 17-32 years. For the $\delta^{13}C$ record the spectrum is strongest at periods ranging between 8-30 years (Figure 16b). For SST this is at periods from 3-17 years (17a), for SOI at periods from 3-10 years (Figure 17b) and finally for IPO at periods between 40-50 years (17c).

Though previous studies have shown a strong link between SST and tropical cyclones and this study shows a positive relationship between tropical cyclones and $\delta^{18}O$, no strong similarities are seen between SST and $\delta^{18}O$. This may be caused by environmental influences on tropical cyclone genesis other than SST, such as surface air pressure, low-level relative vorticity, and deep-tropospheric vertical wind shear (Holland, 1997; Ramsay et al., 2008). In previous studies, $\delta^{13}C$ and SOI have been seen to covary (Frappier et al., 2002; Frappier et al., 2007). In this study a long-term relationship appears to be present between $\delta^{13}C$, SOI and SST. All three wavelet power spectra show the presence of an 8 yr period between 1901-1910 and in 2005 and a 10 yr period between 1975-1985. The wavelet power spectrum of IPO shows similar periods, though less strongly. The short-term variations may have been lost in the $\delta^{13}C$ record due to the lag and yearly groundwater mixing. It may also be that $\delta^{13}C$ is controlled by other environmental factors besides tropical cyclones such as vegetation type, though covariance with $\delta^{18}O$ indicates differently.

The $\delta^{18}O$ depletion record of stalagmite CH2 correlates with instrumental tropical cyclone frequency; in comparison other studies show oxygen isotopes accurately record tropical cyclones in high detail. $\delta^{18}O$ values of tree rings accurately record tropical cyclones in the southeastern USA. Between 1940-1990 all negative excursions in $\delta^{18}O$ correspond to instrumental records for hurricane activity as do most excursions between 1770-1939 (Miller et al., 2006). A monthly $\delta^{18}O$ record from a stalagmite in Belize shows clear negative excursions corresponding to individual tropical cyclone events between 1977-2000. This has primarily been linked to intensity rather than distance (Frappier et al., 2007). An annual $\delta^{18}O$ record from a stalagmite in Queensland shows negative excursions in years with tropical cyclones. The stalagmite records 67% of the tropical cyclones passing within 200

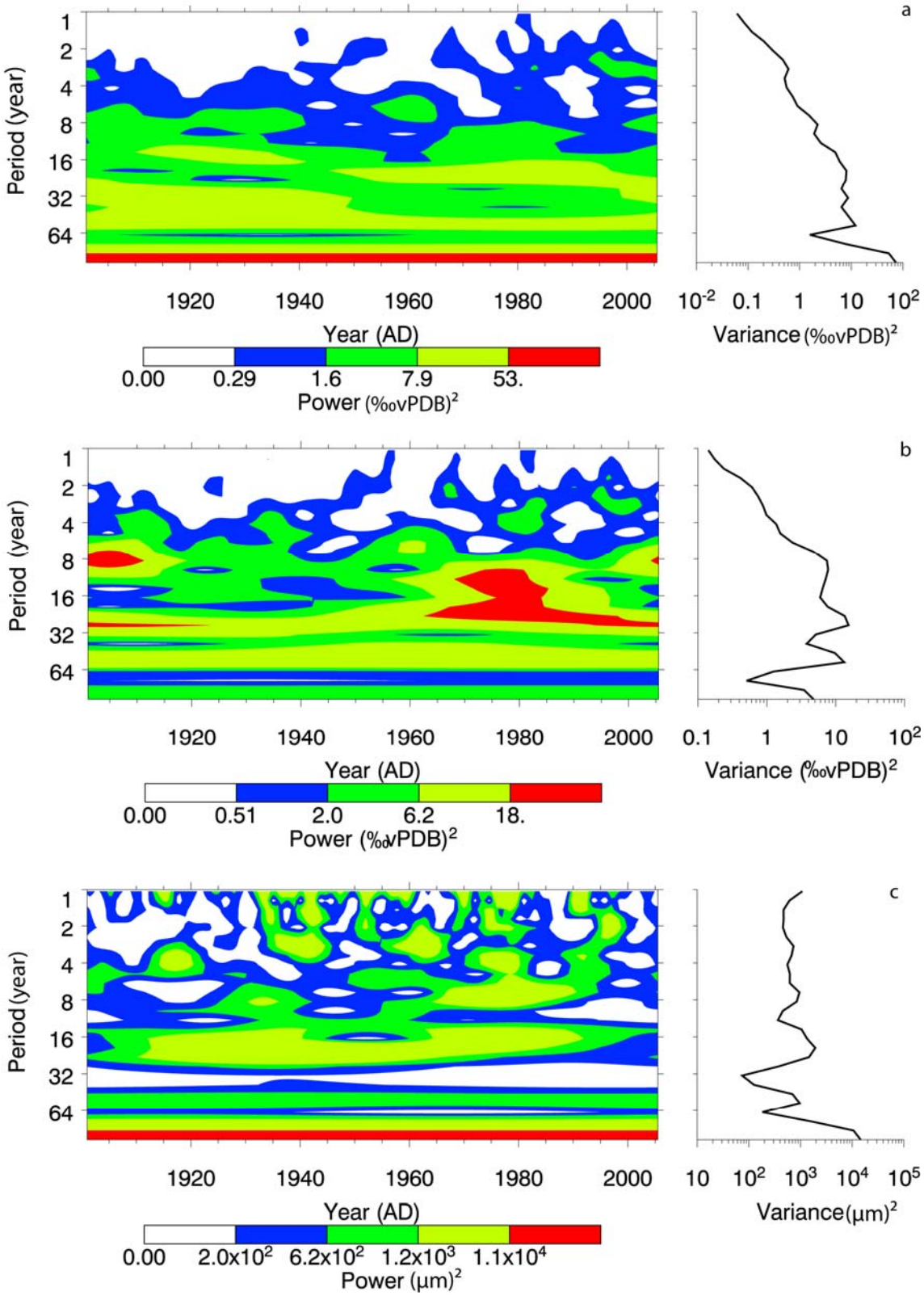

Figure: 16: Wavelet power spectrum of a) the seasonal $\delta^{18}O$ values of CH2 (b) the seasonal $\delta^{13}C$ values of CH2 c) Layer thickness of CH2. Note all analyses are performed on records between 1901-2005 and the contour levels are chosen so that 75%, 50%, 25%, and 5% of the wavelet power is above each level respectively. (Torrence and Compo, 1998)

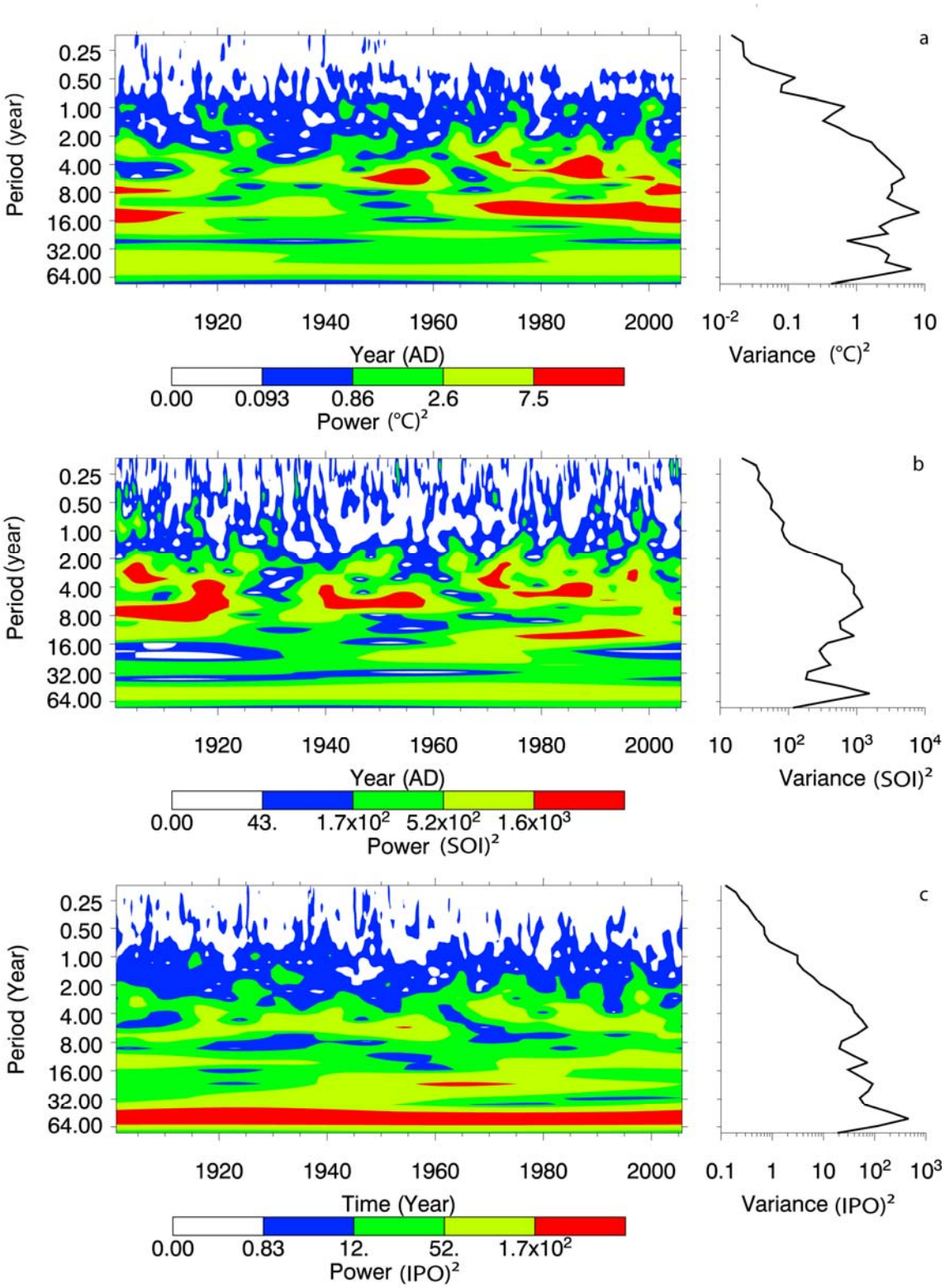

Figure 17: Wavelet power spectrum of a) SST (Niño-4 area) b) Southern Oscillation Index c) Interdecadal Pacific Oscillation. Note all analyses are performed on records between 1901-2005 and the contour levels are chosen so that 75%, 50%, 25%, and 5% of the wavelet power is above each level respectively. (Torrence and Compo, 1998)

km of the cave in the last 100 years. The remaining 33% were either too small or too short-lived to be recorded (Nott et al., 2007). In comparison, CH2 gives an annual $\delta^{18}O$ record with positive correlation to tropical cyclone frequency between 1955-2005. Though the lag and possible mixing diminish the use for individual tropical cyclones, trends in tropical cyclone frequency are recorded and CH2 can be used to determine long term trends in tropical cyclone activity.

Conclusion

Peat core Qui-1 and stalagmite CH2 show a high potential for tropical cyclone reconstructions. The peat core accurately recorded environmental summer temperatures from 1907 until 1949, after which reconstructed MAT shows a cooling trend whilst instrumental temperatures remain stable. Stable isotopes in CH2 will be useful for trends in tropical cyclones, due to their correlation with tropical cyclone frequency. However, due to the lag, identification of individual events will be difficult. Tropical cyclone frequency appears not to be the only factor controlling $\delta^{18}O$. Covariance between carbon and oxygen isotopes in the stalagmite indicates both are controlled by comparable environmental factors such as tropical cyclone activity. Some long-term relationship exists between SST of Niño-4 & SOI and the isotopic composition of CH2. To accurately reconstruct tropical cyclones and compare the two records further research is needed. Hydrogen isotopes from core samples should be compared to the tropical cyclone dataset and a more accurate relationship should be established between $\delta^{18}O$ values from a stalagmite and tropical cyclones.

Acknowledgements

I would like to thank my supervisor Jordahna Haig at James Cook University, Cairns, who has provided me with constant support, assistance and motivation. In addition I would like to thank my two other supervisors at Utrecht University: Els van Soelen for guidance and assistance, and Gert-Jan Reichart for motivation and support. Furthermore I would like to thank Jort Ossebaar at NIOZ for his assistance with the GDGT analysis. Finally, many thanks to Merel Sap, Rolande Dekker, Marieke Lammers, Cornelia Blaga, Maurits Horikx and my parents for support and insightful discussions.

Appendix 1:

Chemical structures of the branched glycerol dialkyl glycerol tetraether (GDGT) membrane lipids

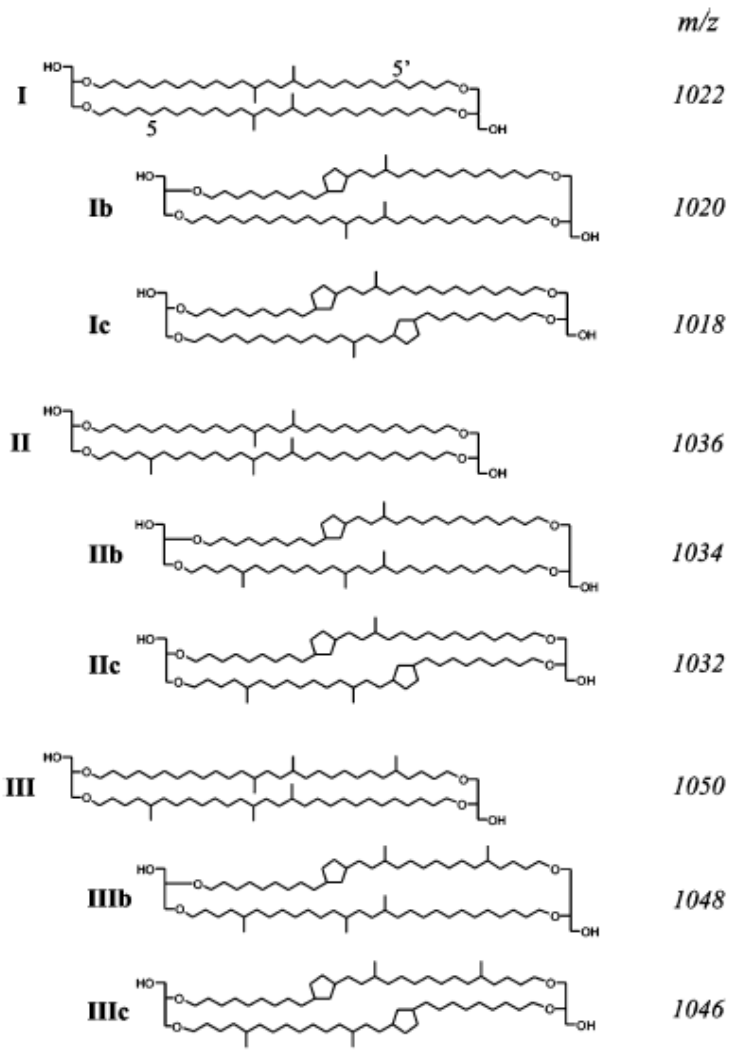

(Weijers et al., 2007)

References

AICHNER, B., HERZSCHUH, U., WILKES, H., VIETH, A. & BÖHNER, J. (2010) δD values of n-alkanes in Tibetan lake sediments and aquatic macrophytes - A surface sediment study and application to a 16ka record from Lake Koucha. *Organic Geochemistry,* 41**,** 779-790.

ALLAN, R. J. (1988) El Niño Southern Oscillation influences in the Australasian region. *Progress in Physical Geography,* 12**,** 313-348.

BAINES, G. B. K. & MCLEAN, R. F. (1976) Sequential studies of hurricane deposit evolution at Funafuti atoll. *Marine Geology,* 21.

BASHER, R. E. & ZHENG, X. (1995) Tropical cyclones in the southwest Pacific: spatial patterns and relationships to Southern Oscillation and sea surface temperature. *Journal of Climate,* 8**,** 1249-1260.

BETANCOURT, J. L., GRISSINO-MAYER, H. D., SALZER, M. W. & SWETNAM, T. W. (2002) A test of "Annual resolution" in stalagmites using tree rings. *Quaternary Research,* 58**,** 197-199.

BOM Australian Bureau of Meteorology (2010) *Climate Data Online.* Accessed:12-02-2010, http://www.bom.gov.au/climate/

BROOK, G. A., RAFTER, M. A., RAILSBACK, L. B., SHEEN, S. W. & LUNDBERG, J. (1999) A high-resolution proxy record of rainfall and ENSO since AD 1550 from layering in stalagmites from Anjohibe Cave, Madagascar. *Holocene,* 9**,** 695-705.

CHAN, J. C. L. (1985) Tropical cyclone activity in the northwest Pacific in relation to the El Nino/Southern Oscillation phenomenon. *Monthly Weather Review,* 113**,** 599-606.

DENNISTON, R. F., GONZÁLEZ, L. A., BAKER, R. G., ASMEROM, Y., REAGAN, M. K., EDWARDS, R. L. & ALEXANDER, E. C. (1999) Speleothem evidence for Holocene fluctuations of the prairie-forest ecotone, north-central USA. *Holocene,* 9**,** 671-676.

DONNELLY, J. P., BRYANT, S. S., BUTLER, J., DOWLING, J., FAN, L., HAUSMANN, N., NEWBY, P., SHUMAN, B., STERN, J., WESTOVER, K. & WEBB III, T. (2001a) 700 yr sedimentary record of intense hurricane landfalls in Southern New England. *Bulletin of the Geological Society of America,* 113**,** 714-727.

DONNELLY, J. P., ROLL, S., WENGREN, M., BUTLER, J., LEDERER, R. & WEBB III, T. (2001b) Sedimentary evidence of intense hurricane strikes from New Jersey. *Geology,* 29**,** 615-618.

DONNELLY, J. P. & WOODRUFF, J. D. (2007) Intense hurricane activity over the past 5,000 years controlled by El Niño and the West African monsoon. *Nature,* 447**,** 465-468.

DORALE, J. A., EDWARDS, R. L., ITO, E. & GONZALEZ, L. A. (1998) Climate and Vegetation History of the Midcontinent from 75 to 25 ka: A Speleothem Record from Crevice Cave, Missouri, USA. *Science,* 282**,** 1871-1874.

DORALE, J. A., GONZÁLEZ, L. A., REAGAN, M. K., PICKETT, D. A., MURRELL, M. T. & BAKER, R. G. (1992) A High-Resolution Record of Holocene Climate Change in Speleothem Calcite from Cold Water Cave, Northeast Iowa. *Science,* 258**,** 1626-1630.

DORALE, J. A. & LIU, Z. (2009) Limitations of hendy test criteria in judging the paleoclimatic suitability of speleothems and the need for replication. *Journal of Cave and Karst Studies,* 71**,** 73-80.

EMANUEL, K., SUNDARARAJAN, R. & WILLIAMS, J. (2008) Hurricanes and global warming: Results from downscaling IPCC AR4 simulations. *Bulletin of the American Meteorological Society,* 89**,** 347-367.

EPA The State of Queensland - Environmental Protection Agency (2002) *Danbulla–Lake Tinaroo Management Strategy*.

FAIRCHILD, I. J., BORSATO, A., TOOTH, A. F., FRISIA, S., HAWKESWORTH, C. J., HUANG, Y., MCDERMOTT, F. & SPIRO, B. (2000) Controls on trace element (Sr-Mg) compositions of carbonate cave waters: implications for speleothem climatic records. *Chemical Geology,* 166**,** 255-269.

FAIRCHILD, I. J. & TREBLE, P. C. (2009) Trace elements in speleothems as recorders of environmental change. *Quaternary Science Reviews,* 28**,** 449-468.

FAN, D. & LIU, K.-B. (2008) Perspectives on the linkage between typhoon activity and global warming from recent research advances in paleotempestology. *Chinese Science Bulletin,* 53**,** 2907-2922.

FLAY, S. & NOTT, J. (2007) Effect of ENSO on Queensland seasonal landfalling tropical cyclone activity. *International Journal of Climatology,* 27**,** 1327-1334.

FLEITMANN, D., BURNS, S. J., NEFF, U., MUDELSEE, M., MANGINI, A. & MATTER, A. (2004) Palaeoclimatic interpretation of high-resolution oxygen isotope profiles derived from annually laminated speleothems from Southern Oman. *Quaternary Science Reviews,* 23**,** 935-945.

FRAPPIER, A., SAHAGIAN, D., GONZÁLEZ, L. A. & CARPENTER, S. J. (2002) El Niño events recorded by stalagmite carbon isotopes. *Science,* 298**,** 565.

FRAPPIER, A. B. (2008) A stepwise screening system to select storm-sensitive stalagmites: Taking a targeted approach to speleothem sampling methodology. *Quaternary International,* 187**,** 25-39.

FRAPPIER, A. B., SAHAGIAN, D., CARPENTER, S. J., GONZÁLEZ, L. A. & FRAPPIER, B. R. (2007) Stalagmite stable isotope record of recent tropical cyclone events. *Geology,* 35**,** 111-114.

GCOS Global Climate Observing System - Working Group on Surface Pressure (2009) *Climate Timeseries.* Accessed:23-07-2010, http://www.esrl.noaa.gov/psd/gcos_wgsp/Timeseries/Nino4/

GEDZELMAN, S., LAWRENCE, J., GAMACHE, J., BLACK, M., HINDMAN, E., BLACK, R., DUNION, J., WILLOUGHBY, H. & ZHANG, X. (2003) Probing hurricanes with stable isotopes of rain and water vapor. *Monthly Weather Review,* 131**,** 1112-1127.

GEDZELMAN, S. D. & LAWRENCE, J. R. (1982) The isotopic composition of cyclonic precipitation (Palisades,NY). *Journal of Applied Meteorology,* 21**,** 1385-1404.

GENTY, D., BAKER, A., MASSAULT, M., PROCTOR, C., GILMOUR, M., PONS-BRANCHU, E. & HAMELIN, B. (2001) Dead carbon in stalagmites: Carbonate bedrock paleodissolution vs. ageing of soil organic matter. Implications for 13C variations in speleotherms. *Geochimica et Cosmochimica Acta,* 65**,** 3443-3457.

GENTY, D., BLAMART, D., GHALEB, B., PLAGNES, V., CAUSSE, C., BAKALOWICZ, M., ZOUARI, K., CHKIR, N., HELLSTROM, J., WAINER, K. & BOURGES, F. (2006) Timing and dynamics of the last deglaciation from European and North African [delta]13C stalagmite profiles--comparison with Chinese and South Hemisphere stalagmites. *Quaternary Science Reviews,* 25**,** 2118-2142.

GOEDE, A. (1994) Continuous early last glacial palaeoenvironmental record from a tasmanian speleothem based on stable isotope and minor element variations. *Quaternary Science Reviews,* 13**,** 283-291.

GRANT, A. P. & WALSH, K. J. E. (2001) Interdecadal variability in north-east Australian tropical cyclone formation. *Atmospheric Science Letters,* 2**,** 9-17.

GRIFFITHS, M. L., DRYSDALE, R. N., GAGAN, M. K., FRISIA, S., ZHAO, J. X., AYLIFFE, L. K., HANTORO, W. S., HELLSTROM, J. C., FISCHER, M. J., FENG, Y. X. & SUWARGADI, B. W. (2010) Evidence for Holocene changes in Australian-Indonesian monsoon rainfall from

stalagmite trace element and stable isotope ratios. *Earth and Planetary Science Letters,* 292**,** 27-38.

HAYNE, M. & CHAPPELL, J. (2001) Cyclone frequency during the last 5000 years at Curacoa Island, north Queensland, Australia. *Palaeogeography, Palaeoclimatology, Palaeoecology,* 168**,** 207-219.

HELLSTROM, J., MCCULLOCH, M. & STONE, J. (1998) A detailed 31,000-year record of climate and vegetation change, from the isotope geochemistry of two New Zealand speleothems. *Quaternary Research,* 50**,** 167-178.

HENDY, C. H. (1971) The isotopic geochemistry of speleothems-I. The calculation of the effects of different modes of formation on the isotopic composition of speleothems and their applicability as palaeoclimatic indicators. *Geochimica et Cosmochimica Acta,* 35**,** 801-824.

HENDY, C. H. & WILSON, A. T. (1968) Palaeoclimatic Data from Speleothems. *Nature,* 219**,** 48-51.

HOLLAND, G. J. (1997) The maximum potential intensity of tropical cyclones. *Journal of the Atmospheric Sciences,* 54**,** 2519-2541.

ITO, M., ISHIGAKI, A., NISHIKAWA, T. & SAITO, T. (2001) Temporal variation in the wavelength of hummocky cross-stratification: Implications for storm intensity through Mesozoic and Cenozoic. *Geology,* 29**,** 87-89.

KERSHAW, A. P. (1971) A Pollen Diagram from Quincan Crater, North-East Queensland, Australia. *New Phytologist,* 70**,** 669-681.

KULESHOV, Y., FAWCETT, R., QI, L., TREWIN, B., JONES, D., MCBRIDE, J. & RAMSAY, H. (2010) Trends in tropical cyclones in the South Indian Ocean and the South Pacific Ocean. *Journal of Geophysical Research D: Atmospheres,* 115.

LANDSEA, C. W., HARPER, B. A., HOARAU, K. & KNAFF, J. A. (2006) Can we detect trends in extreme tropical cyclones? *Science,* 313**,** 452-454.

LAURITZEN, S. E. & LUNDBERG, J. (1999) Calibration of the speleothem delta function: An absolute temperature record for the Holocene in northern Norway. *Holocene,* 9**,** 659-669.

LAWRENCE, J. R. (1998) Isotopic spikes from tropical cyclones in surface waters: Opportunities in hydrology and paleoclimatology. *Chemical Geology,* 144**,** 153-160.

LAWRENCE, J. R. & GEDZELMAN, S. D. (1996) Low stable isotope ratios of tropical cyclone rains. *Geophysical Research Letters,* 23**,** 527-530.

LAWRENCE, J. R., GEDZELMAN, S. D., DEXHEIMER, D., CHO, H. K., CARRIE, G. D., GASPARINI, R., ANDERSON, C. R., BOWMAN, K. P. & BIGGERSTAFF, M. I. (2004) Stable isotopic composition of water vapor in the tropics. *Journal of Geophysical Research D: Atmospheres,* 109.

LAWRENCE, J. R., GEDZELMAN, S. D., ZHANG, X. & ARNOLD, R. (1998) Stable isotope ratios of rain and vapor in 1995 hurricanes. *Journal of Geophysical Research D: Atmospheres,* 103**,** 11381-11400.

LEES, W. (1899) *The Goldfields of Queensland,* Atherton, Eacham Historical Society.

LINGE, H., LAURITZEN, S. E., LUNDBERG, J. & BERSTAD, I. M. (2001) Stable isotope stratigraphy of Holocene speleothems: Examples from a cave system in Rana, northern Norway. *Palaeogeography, Palaeoclimatology, Palaeoecology,* 167**,** 209-224.

LIU, K. & FEARN, M. L. (2000) Reconstruction of prehistoric landfall frequencies of catastrophic hurricanes in Northwestern Florida from lake sediment records. *Quaternary Research,* 54**,** 238-245.

MCDERMOTT, F. (2004) Palaeo-climate reconstruction from stable isotope variations in speleothems: a review. *Quaternary Science Reviews,* 23**,** 901-918.

MILLER, D. L., MORA, C. I., GRISSINO-MAYER, H. D., MOCK, C. J., UHLE, M. E. & SHARP, Z. (2006) Tree-ring isotope records of tropical cyclone activity. *Proceedings of the National Academy of Sciences of the United States of America,* 103**,** 14294-14297.

NICHOLLS, N. (1979) A possible method for predicting seasonal tropical cyclone activity in the Australian region. *Monthly Weather Review,* 107**,** 1221-1224.

NICHOLLS, N., COLLINS, D., TREWIN, B. & HOPE, P. (2006) Historical instrumental climate data for Australia - Quality and utility for palaeoclimatic studies. *Journal of Quaternary Science,* 21**,** 681-688.

NICHOLLS, N., LANDSEA, C. & GILL, J. (1998) Recent trends in Australian region tropical cyclone activity. *Meteorology and Atmospheric Physics,* 65**,** 197-205.

NOTT, J., HAIG, J., NEIL, H. & GILLIESON, D. (2007) Greater frequency variability of landfalling tropical cyclones at centennial compared to seasonal and decadal scales. *Earth and Planetary Science Letters,* 255**,** 367-372.

NOTT, J. & HAYNE, M. (2001) High frequency of 'super-cyclones' along the Great Barrier Reef over the past 5,000 years. *Nature,* 413**,** 508-512.

NOTT, J. F. (2003) Intensity of prehistoric tropical cyclones. *Journal of Geophysical Research D: Atmospheres,* 108.

PETERSE, F., KIM, J. H., SCHOUTEN, S., KRISTENSEN, D. K., KOÇ, N. & SINNINGHE DAMSTÉ, J. S. (2009a) Constraints on the application of the MBT/CBT palaeothermometer at high latitude environments (Svalbard, Norway). *Organic Geochemistry,* 40**,** 692-699.

PETERSE, F., SCHOUTEN, S., VAN DER MEER, J., VAN DER MEER, M. T. J. & SINNINGHE DAMSTÉ, J. S. (2009b) Distribution of branched tetraether lipids in geothermally heated soils: Implications for the MBT/CBT temperature proxy. *Organic Geochemistry,* 40**,** 201-205.

PLIMER, I. (1997) *A Journey Through Stone,* Victoria, Reed.

RAMSAY, H. A., LESLIE, L. M., LAMB, P. J., RICHMAN, M. B. & LEPLASTRIER, M. (2008) Interannual variability of tropical cyclones in the Australian region: Role of large-scale environment. *Journal of Climate,* 21**,** 1083-1103.

RASBURY, M. & AHARON, P. (2006) ENSO-controlled rainfall variability records archived in tropical stalagmites from the mid-ocean island of Niue, South Pacific. *Geochemistry, Geophysics, Geosystems,* 7.

SELF, C. A. & HILL, C. A. (2003) How speleothems grow: An introduction to the ontogeny of cave minerals. *Journal of Cave and Karst Studies,* 65**,** 130-145.

SINNINGHE DAMSTÉ, J. S., HOPMANS, E. C., PANCOST, R. D., SCHOUTEN, S. & GEENEVASEN, J. A. J. (2000) Newly discovered non-isoprenoid glycerol dialkyl glycerol tetraether lipids in sediments. *Chemical Communications***,** 1683-1684.

SINNINGHE DAMSTÉ, J. S., OSSEBAAR, J., SCHOUTEN, S. & VERSCHUREN, D. (2008) Altitudinal shifts in the branched tetraether lipid distribution in soil from Mt. Kilimanjaro (Tanzania): Implications for the MBT/CBT continental palaeothermometer. *Organic Geochemistry,* 39**,** 1072-1076.

SPÖTL, C., FAIRCHILD, I. J. & TOOTH, A. F. (2005) Cave air control on dripwater geochemistry, Obir Caves (Austria): Implications for speleothem deposition in dynamically ventilated caves. *Geochimica et Cosmochimica Acta,* 69**,** 2451-2468.

SPÖTL, C., MANGINI, A., FRANK, N., EICHSTÄDTER, R. & BURNS, S. J. (2002) Start of the last interglacial period at 135 ka: Evidence from a high Alpine speleothem. *Geology,* 30**,** 815-818.

THOMPSON, P., SCHWARCZ, H. P. & FORD, D. C. (1976) Stable isotope geochemistry, geothermometry, and geochronology of speleothems from West Virginia. *Geological Society of America Bulletin,* 87**,** 1730-1738.

TORRENCE, C. & COMPO, G. P. (1998) *A Practical Guide to Wavelet Analysis.* Accessed:24-07-2010, http://paos.colorado.edu/research/wavelets/

TREBLE, P., SHELLEY, J. M. G. & CHAPPELL, J. (2003) Comparison of high resolution sub-annual records of trace elements in a modern (1911-1992) speleothem with instrumental climate data from southwest Australia. *Earth and Planetary Science Letters,* 216**,** 141-153.

TREBLE, P. C., CHAPPELL, J., GAGAN, M. K., MCKEEGAN, K. D. & HARRISON, T. M. (2005a) In situ measurement of seasonal δ18O variations and analysis of isotopic trends in a modern speleothem from southwest Australia. *Earth and Planetary Science Letters,* 233**,** 17-32.

TREBLE, P. C., CHAPPELL, J. & SHELLEY, J. M. G. (2005b) Complex speleothem growth processes revealed by trace element mapping and scanning electron microscopy of annual layers. *Geochimica et Cosmochimica Acta,* 69**,** 4855-4863.

TREBLE, P. C., SCHMITT, A. K., EDWARDS, R. L., MCKEEGAN, K. D., HARRISON, T. M., GROVE, M., CHENG, H. & WANG, Y. J. (2007) High resolution Secondary Ionisation Mass Spectrometry (SIMS) δ18O analyses of Hulu Cave speleothem at the time of Heinrich Event 1. *Chemical Geology,* 238**,** 197-212.

TREWIN, B. (2008) *An enhanced tropical cyclone data set from the Australian region. 20th Conference on Climate Variability and Change.* New Orleans, American Meteorological Society.

VERHEYDEN, S., GENTY, D., DEFLANDRE, G., QUINIF, Y. & KEPPENS, E. (2008) Monitoring climatological, hydrological and geochemical parameters in the Père Noël cave (Belgium): Implication for the interpretation of speleothem isotopic and geochemical time-series. *International Journal of Speleology,* 37**,** 221-234.

WALSH, K. J. E. & RYAN, B. F. (2000) Tropical Cyclone Intensity Increase near Australia as a Result of Climate Change. *Journal of Climate,* 13**,** 1.

WATSON, R. T., ZINYOWEYA, M.C., MOSS, R.H. (Ed.) (1996) *Climate Change 1995: Impacts, Adapatations and Migitation of Climate Change: Scientific-Technical Analyses. Contribution of Working Group II to the Second Assessment Teport of the Intergovernmental Panel on Climate Change*, Cambridge University Press.

WEIJERS, J. W. H., SCHOUTEN, S., HOPMANS, E. C., GEENEVASEN, J. A. J., DAVID, O. R. P., COLEMAN, J. M., PANCOST, R. D. & SINNINGHE DAMSTÉ, J. S. (2006) Membrane lipids of mesophilic anaerobic bacteria thriving in peats have typical archaeal traits. *Environmental Microbiology,* 8**,** 648-657.

WEIJERS, J. W. H., SCHOUTEN, S., VAN DEN DONKER, J. C., HOPMANS, E. C. & SINNINGHE DAMSTÉ, J. S. (2007) Environmental controls on bacterial tetraether membrane lipid distribution in soils. *Geochimica et Cosmochimica Acta,* 71**,** 703-713.

WHITE, W. B. (2004) Paleoclimate Records from Speleothems in Limestone Caves. IN SASOWSKY, I. D. & MYLROIE, J. (Eds.) *Studies of cave sediments: physical and chemical records of paleoclimate.* Kluwer Academic/Plenum Publishers, New York, pp. 135-176

WHITE, W. B. (2007) Cave sediments and paleoclimate. *Journal of Cave and Karst Studies,* 69**,** 76-93.

WILLMOTT, W. F. & TREZISE, D. L. (1989) *Rocks and Landscapes of the Chillagoe District,* Brisbane, Queensland Department of Mines.